thermo

MDPI

Article

Molecular, Crystalline, and Microstructures of Lipids from *Astrocaryum* Species in Guyana and Their Thermal and Flow Behavior

Shaveshwar Deonarine [1], Navindra Soodoo [1], Laziz Bouzidi [1], R. J. Neil Emery [2], Sanela Martic [3] and Suresh S. Narine [1,*]

[1] Centre for Biomaterials Research, Departments of Physics and Astronomy and Chemistry, Trent University, 1600 West Bank Drive, Peterborough, ON K9L 0G2, Canada; shaveshwardeonarine@trentu.ca (S.D.); navindrasoodoo@trentu.ca (N.S.); lazizbouzidi@trentu.ca (L.B.)
[2] Department of Biology, Trent University, 1600 West Bank Drive, Peterborough, ON K9L 0G2, Canada; nemery@trentu.ca
[3] Forensic Science, Trent University, 1600 West Bank Drive, Peterborough, ON K9L 0G2, Canada; sanelamartic@trentu.ca
* Correspondence: sureshnarine@trentu.ca; Tel.: +1-705-748-1011; Fax: +1-705-750-2786

Abstract: The phase behavior of lipids extracted from *Astrocaryum vulgare* (AV) and *Astrocaryum aculeatum* (AA) pulp and kernels and their microstructural, thermal and flow properties were studied. The lipid profiles, crystal structures, microstructures, thermal stabilities and flow behaviors of these lipids provided important structure–function information that are useful to assess potential applications in the food, cosmetic and pharmaceutical industries. AV and AA fruits were sourced from the lowlands and rainforests, respectively, of Guyana. AV and AA pulp oils (AVP and AAP) were distinguished from each other in composition and unsaturation, with AVP oils being predominated by a di-unsaturated TAG (2-(palmitoyloxy)propane-1,3-diyl dioleate (POO)) and AAP oils predominated by propane-1,2,3-triyl trioleate (OOO); there were unsaturation levels of 65% and 80%, respectively. The main fatty acids in AVP oils were oleic, palmitic and stearic; for AAP, these were oleic, linoleic, palmitic and stearic. The kernel fats of AV and AA were similar in composition and had saturation levels of 80%, being mainly comprised of tri-saturated TAGs propane-1,2,3-triyl tridodecanoate (LLL) and 3-(tetradecanoyloxy)propane-1,2-diyl didodecanoate (LML). The onset of mass loss $\left(T_{5\%}^{on}\right)$ of AV and AA pulp oils were similar at 328 ± 6 °C, which were 31 °C ± 9 higher compared to that of the kernel fats, which demonstrated similar $T_{5\%}^{on}$ = 293 ± 7 °C. AA and AV pulp oils were liquid at room temperature, with melting points of −5 ± 1 °C and 3 ± 1 °C, respectively; both kernel fats were solid at room temperature, packing in β′ (90% of crystals) and β (10% of crystals) polymorphic forms and melting almost identically at 30 ± 1 °C. Pulp oils demonstrated sporadic nucleation at the onset of crystallization with slow growth into rod-shaped crystallites, leading to an approximately 50% degree of crystallization at undercooling of approximately 40K. Nucleation for kernel fats was instantaneous at undercooling of approximately 23K, demonstrating a spherulitic growth pattern incorporating crystalline lamella and a 90% degree of crystallization. Kernel fats and pulp oils demonstrated Newtonian flow behavior and similar dynamic viscosity in the melt, approximately 28.5 mPa·s at 40 °C. The lipid profiles of AVP and AAP oils were dominated by unsaturated TAGs, suggesting potential nutrition and health benefits, particularly compared to other tropical oils with higher saturation levels, such as palm oil. AAP oil in particular is as unsaturated as olive oil, contains high levels of beta carotene and provides a unique flavor profile. The AAK and AVK lipid profiles and phase transformation indicate potential for applications where a high solid fat content and medium-chain fatty acids are required. Their high lauric and myristic acid content makes them similar to industrially important tropical oils (coconut and palm kernel), suggesting their use in similar formulations. The melting point and plasticity of the kernel fats are similar to that of cocoa and shea butters, suggesting use as replacements in cosmetics, foods and confections. There is, however, the need to better understand their nutritional status and effects on health.

Citation: Deonarine, S.; Soodoo, N.; Bouzidi, L.; Emery, R.J.N.; Martic, S.; Narine, S.S. Molecular, Crystalline, and Microstructures of Lipids from *Astrocaryum* Species in Guyana and Their Thermal and Flow Behavior. *Thermo* **2024**, *4*, 140–163. https://doi.org/10.3390/thermo4010009

Academic Editors: Santiago Aparicio, Johan Jacquemin, Steve Lustig, Andrew S. Paluch and William E. Acree, Jr.

Received: 7 January 2024
Revised: 10 February 2024
Accepted: 4 March 2024
Published: 12 March 2024

Keywords: Guyana; *Astrocaryum vulgare*; *Astrocaryum aculeatum*; thermal behavior; molecular profile; crystal structure; microstructure; flow behavior

1. Introduction

In recent years, the demand for naturally sourced ingredients over chemically processed alternatives has significantly increased, mainly due to a rising focus on healthy lifestyles, environment and sustainability [1,2]. Consequently, the food, pharmaceutical and cosmetic industries have invested in the sourcing of natural ingredients for their products [3]. Lipids are a particularly studied component of the product formulations used in these industries [4]. In addition to increasing the solubility of the active ingredients [5] and imbuing foods and cosmetics with flavor and texture, lipids are used to provide important dietary components such as essential fatty acids, fat-soluble vitamins and other bioactives. Consequently, lipids are widely incorporated as active ingredients in cosmetics and pharmaceuticals [6].

Tropical habitats such as the rainforests and swamps of the Guiana Shield and the Amazonian basin are full of oleaginous species that can potentially provide functional and bioactive lipids for food, cosmetic and pharmaceutical materials [7]. For many such species, the fruits and associated lipids are already traditionally used in many aspects of the local communities' lives, including as food and medicine, and can form part of their cultural and economic fabric [8,9]. Most of the oleaginous plants that thrive in these environments [7] are of particular interest, as their lipids often possess distinctive physical, chemical and bioactive properties, making them of potential interest in varied high-value foods, pharmaceuticals and cosmetics [7,10,11]. Although research in the area is increasing, these materials are generally not thoroughly or at all studied by mainstream academia. Nonetheless, currently, in the food industry, lipids from recognized tropical oleaginous plants are used for cooking, delivering unique nutritional benefits, flavors and textures [7,11]. In pharmaceuticals, they are employed in drug formulations and delivery systems [5,12]. The cosmetic industry utilizes them for their moisturizing and emollient properties in products such as lotions and creams [13–15].

Astrocaryum vulgare (AV, Awara in Guyana and Tucumã do Amazonas in Brazil) and *Astrocaryum aculeatum* (AA, Kuru in Guyana and Tucumã do Para in Brazil) are two related tropical plants of the *Arecaceae* family that have been the subject of ongoing research because of the reported nutritional and medicinal properties of their fruits and oils [16]. Their fruits share similar morphology, comprising of a fibrous mesocarp (pulp) surrounding a hard pyrene (seed) that houses the endocarp (kernel). The pulp, the main edible part, constitutes 50% of the overall mass of the fresh fruit [17]. It is fleshy with a fibrous or mucilaginous and oily consistency and a tasty and sweet flavor when ripe. The fruits contain significant amounts of carbohydrates (7–20%), fibers (11–30%) and lipids (25–50%) and relatively small amounts of proteins (3–10%) and minerals (2–3%) [18–21]. The kernel accounts for 50% of the seed [17].

It is reported that the oils extracted from *Astrocaryum vulgare* pulp (AVP) and *Astrocaryum aculeatum* pulp (AAP) are similar in composition; so are the fats from their kernels (AVK and AAK, respectively). However, pulp oils and kernel fats have distinctively different chemical compositions [8,22,23]. Notably, the pulp oils are highly unsaturated, including ω-3, ω-6 and ω-9 fatty acids [21,24], whereas the kernel oils are highly saturated fats [23,25]. At room temperature, AVP and AAP oils are liquid, with melting points (T_m) of −5 °C and 3 °C, respectively, whereas AVK and AAK oils are solid at room temperature, with Tm = 30 °C. AVP oil comprises up to 72% unsaturated fatty acids (UFAs), with the predominance of oleic acid (C18:1), reported as constituting between 63 and 75% of the total fatty acids [26,27]. Palmitic acid (C16:0) is the dominant saturated fatty acid (SFA) found in AVP oil, making up 23–26% of the total. Other fatty acids found in AVP include α-linolenic (C18:3), linoleic (C18:2) and stearic (C18:0) acids [22,28,29]. The oil from AAP

has a similar fatty acid profile, with up to 74% UFAs that are also dominated by oleic acid (47–64%) and palmitic acid as the dominant fatty acid (10–14) [30,31]. AVK and AAK oils are highly saturated, with lauric acid (C12:0) and myristic acid (C14:0) dominating in both. The reported lauric, myristic and palmitic acid contents in AVK oil are 48–54%, 24–26% and 5–6%, respectively [22,32,33], and in AAK oil they are 52–58%, 14–18% and 7–10%, respectively [32].

The pulp oils and kernel fats [34] of AV and AA contain fat-soluble bioactive compounds including carotenoids [35], phenolic compounds [36] and sterols [35]. In vitro experiments indicate antimicrobial, antifungal [37], anti-inflammatory [35], antiproliferative [38], cytoprotective [39], skin-protective [7] and antioxidant [36,40,41] activity for these lipids.

Despite their nutritional and health-promoting properties, the knowledge and use of these Astrocaryum lipids are mostly confined to their native regions (Brazil and Guyana). This limited recognition hinders their broader application in industries that could benefit from their inherent physical and chemical properties, including their antimicrobial, anti-inflammatory, and antioxidant activities. With further research, these oils and fats could potentially be significant parts of nutritious foods or functional cosmetics, with added health and therapeutic advantages. Enhancing global awareness and facilitating their integration into international markets can help global food security and address the rising demand for naturally derived products. Although studies have been performed on these tropical palm fruits, the key aspects of AV and AA pulp oils and kernel fats remain largely unexplored [8]. For instance, the TAG profiles of AVP oil and AVK fat are reported [23,25] but not those of AAP oil and AAK fat. Investigations of the physical properties of these fats and oils, including thermal transition behavior, crystal structure, microstructure and flow behavior, report inconsistent values among the few reported studies [7,32,36]. Furthermore, most studies concern Brazilian plants, which may differ from similar species present in other environments. Based on a comprehensive search of the literature and to the best of our knowledge, there are no published studies on the structural and molecular properties of lipids extracted from the fruits of AV and AA species found in Guyana's rainforest and swamps. This work investigates the structure at multiple length scales: molecular, crystalline and microstructural and the thermal and flow properties of the pulp oils and kernel fats extracted via the cold pressing of AV and AA fruits the forests and swamps of Guyana.

The lipid molecular composition was compared to the reported literature on these oils and contrasted against similar well-known plant oils, such as palm oil, shea butter, cocoa butter, *Carapa guianensis* (crabwood in Guyana and andiroba in Brazil) oil and coconut oil. The relationships between molecular composition, crystalline packing and developed microstructure were also used to explain thermal and flow behaviors. Based on this analysis, several potential uses of oils from the *Astrocaryum* species sourced from Guyana were recommended.

2. Materials and Methods

2.1. Sample Collection, Processing and Handling

Fruits from AV and AA were hand-picked in May 2023 directly from Guyana's forests and swamps, specifically Administrative Regions 1 and 2. The fresh fruits were individually inspected. Fruits that were unripe or presented signs of blemishes, damage or decay were discarded. The remaining stems, twigs and leaves were removed, then the fruits were washed with distilled water. Figure 1 shows AV and AA fruit samples. The pulps were separated from the seeds using stainless steel knives and peelers, and kernels were obtained by cross-sectionally splitting the seeds using a knife and hammer. Both fresh pulps and kernels, placed in rectangular aluminum pans (26 cm × 20 cm × 6 cm) in a 0.5–1 cm-thick layer, were dried under ambient environmental conditions and then pulverized to a particle size of approximately 10 µm using a high speed multifunctional comminutor (Seeutek, CA, USA). The samples were then stored in sealed bags (Ziploc®, SC Johnson,

Brantford, ON, Canada) at room temperature (25 °C). The drying process and kinetics for these materials, as well as details on the extraction of the oils and fats, are reported in our previous publication [17].

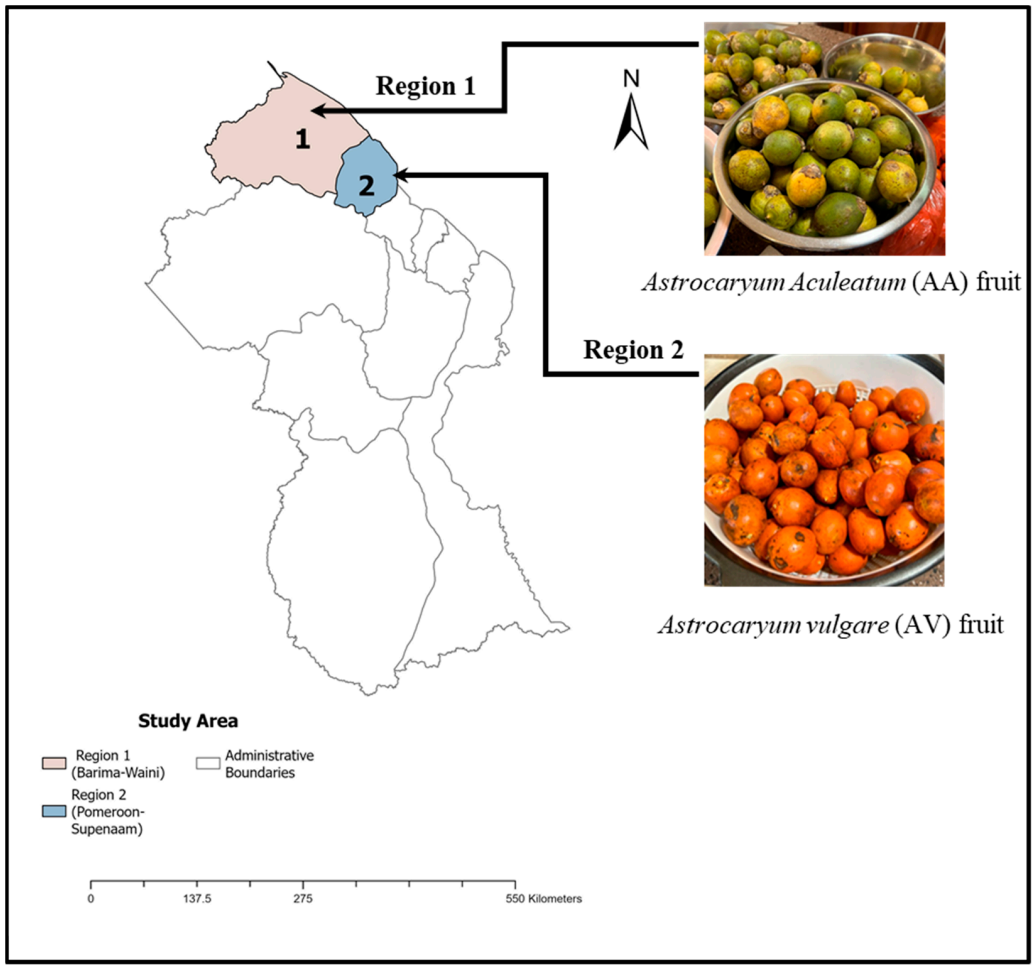

Figure 1. Map of Guyana showing the administrative regions where the fruits *Astrocaryum vulgare* (AV) and *Astrocaryum aculeatum* (AA) were collected.

2.2. Oil Extraction

The oils and fats were extracted from the dried, pulverized pulp and kernels by mechanical pressing using a 1500-Watt portable cold-press oil expeller (CGOLDENWALL, Beijing, China), as described in Deonarine et al. [17]. The temperature of the sample in the expeller was monitored using a Fluke 568 infrared thermometer (ITM Instruments, York, ON, Canada). AVK and AAK oils were extracted at higher temperatures because these lipids fully melt at 35 °C and are not easily extractable in the solid state. In this case, the expeller was pre-heated to 50 °C using the built-in temperature controller to melt the fat in situ and allow easy oil extraction from the kernels. The friction during extraction increased the temperature to up to 80 °C. At 50 °C, no alteration of the lipid and non-lipid components is expected; however, at temperatures close to 80 °C, some non-lipid components may be lost. This assertion is to be verified by alternate low-temperature extraction methods, such as supercritical carbon dioxide extraction. The extracted fats and oils were stored in glass jars and at 4 °C until the time of analysis.

2.3. Fourier-Transform Infrared Spectroscopy (FTIR)

Attenuated total reflectance Fourier-transform infrared spectroscopy (FTIR-ATR) spectra were collected using a Thermo Scientific Nicolet 380 FTIR spectrometer (Thermo Elec-

tron Scientific Instruments LLC, Swedesboro, NJ, USA) equipped with a single reflection diamond ATR accessory. Samples were mounted on the diamond ATR crystal and measurements were performed at room temperature. A total of 128 scans were collected for each sample over a range of 400 to 4000 cm^{-1} at a spectral resolution of 4 cm^{-1}. ATR correction was performed after each data acquisition. OMNIC software (Thermo Scientific Inc., Waltham, MA, USA) (https://www.thermofisher.com/order/catalog/product/INQSOF018) was used for all spectral manipulations.

2.4. Electrospray Ionization Mass Spectrometry (ESI-MS)

Electrospray ionization mass spectrometry (ESI-MS) was performed using a Thermo QExactive Orbitrap mass spectrometer (Thermo Fisher Scientific, San Jose, CA, USA) in the positive ion mode. Samples were injected using a syringe infusion pump (Harvard Apparatus, Holliston, MA, USA) and analyzed using an instrument resolution of 17,500. The ESI source temperature was 320 °C and the scan rate was 12.5 scan/s. Methanol (HPLC grade; VWR, Mississauga, ON, Canada) was used as the source of hydrogen ion and chloroform (HPLC grade; VWR, Mississauga, ON, Canada) was used to dissolve the lipid analyte. Samples (1 ppm wt./v) were prepared using 70:30 (v/v) chloroform:methanol mixtures. ESI-MS was used to determine the lipid profiles of AV and AA pulp oils and kernel fats, specifically triacylglycerols (TAGs), diacylglycerols (DAGs) and monoacylglycerols (MAGs). The MS data were processed using the Qual Browser tool of the Thermo Xcalibur software version 3.1 (Thermo Scientific, Waltham, MA, USA). The NIST, Lipid Maps®, MetaboQuest and XCMS online databases were used for identification of the components based on ion mass. The components were further assigned into structural isomers using data mined from the published literature [25,26]. The relative intensities for each class of TAGs, DAGs and MAGs were calculated by dividing the individual molecule intensities by the sum of intensities.

2.5. Thermogravimetric Analysis (TGA)

Thermogravimetric analysis (TGA) was performed on a TGA Q500 (TA Instruments, Newcastle, DE, USA). The sample (10–15 mg) was heated on a platinum pan from 25 °C to 600 °C at 10 °C/min under a nitrogen flow of 60.0 mL/min. The thermal stability of the compounds was characterized by the onset temperature of mass loss taken at 5% w/w ($T^{on}_{5\%}$) following a typical protocol. The derivative of the TGA (DTG) was calculated from the experimental TGA to assess the mechanisms of mass loss, as indicated by the DTG peak temperature (T_D) and maximum rate of degradation.

2.6. Differential Scanning Calorimetry (DSC)

The thermal transition behavior of the four lipids was determined using a Q200 DSC (TA Instruments, Newcastle, DE, USA) equipped with a refrigerated cooling system and calibrated with pure indium. Preliminary measurements were performed to establish an appropriate DSC measurement temperature range and ensure that the crystallization and melting of the materials were completed. The limit temperature was chosen when the fully melted material, as indicated by its melting offset, was followed by a satisfactory stable heat flow plateau. A 10–15 °C plateau is considered sufficient to confirm complete melting. In our case, the highest measured melting offset was 34 °C for the kernel fats and 11 °C for the pulp oils. The plateau was extended to 60 °C to allow not only confirmation of complete melting but also for the best analysis of the events detected by DSC during the transformation path. Samples (4–6 mg) in hermetic aluminum pans was equilibrated at 60 °C for 5 min to erase thermal history, then cooled at a prescribed rate (5 °C/min) down to −80 °C, where they were held isothermally for 5 min to record the crystallization behavior and then heated back to 60 °C at 10 °C/min to investigate the melting behavior. The DSC thermograms were analyzed using Thermal Advantage (TA) universal analysis software (TA Advantage v5.5.24).

2.7. X-ray Diffraction (XRD)

X-ray diffraction (XRD) measurements were performed on an Empyrean X-ray diffractometer equipped with Cu-Kα radiation and a PIXcel3D detector (PANalytical B.V., Lelyweg, The Netherlands). The sample was melted at 40 °C to facilitate easy and uniform loading into a preheated 1 mm glass capillary tube (Hampton Research, Aliso Viejo, CA, USA), left to crystallize at RT = 18 °C for 7–10 days, then measured at RT. The diffractometer was operated at 45 kV and 40 mA. The XRD patterns were recorded between 0.5° and 36° (2θ) in 0.013° steps, with 250 s intervals. The procedure was automated and controlled by PANalytical's Data Collector (V 3.0a) software. The regions of wide-angle x-ray diffraction scattering (WAXD, 2θ > 15°) and small-angle x-ray diffraction scattering (SAXD, 2θ < 15°), which fingerprint the sub cell structures and the molecules layer order along the normal direction, respectively, were analyzed like other fatty compounds.

2.8. Polarized-Light Microscopy (PLM)

A Leica DM2500P polarized-light microscope (PLM) (Leica Microsystems, Wetzlar, Germany) fitted with a Leica DFC420C digital camera was used for the microstructure studies. A Linkam LS 350 temperature-controlled stage (Linkam Scientific Instruments, Tadworth, Surrey, UK) fitted to the PLM was used to thermally condition the samples. A small droplet of the sample was carefully pressed between a preheated glass slide and coverslip, ensuring a uniform thin layer. The sample was heated to 60 °C at a rate 10 °C/min to erase crystal memory, then cooled down to −65 °C at 5 °C/min. Temperature-resolved images were taken during cooling at 5 °C intervals at 50×, 100× and 200× magnifications. The temperature at which the first growth centers, observed as "black spots", occur is recorded as the induction temperature of crystallization (*Tind*).

2.9. Viscosity and Flow Behavior

Viscosity and flow behavior were determined on a computer-controlled AR2000ex rheometer (TA Instruments, DE, USA) using a standard 40 mm 2° steel cone geometry (SIN 511406.901, TA Instruments) under an air bearing pressure of 27 psi. Temperature control was achieved using a Peltier plate (AR Series, TA Instruments) with an accuracy of 0.1 °C. The shear rate–shear stress experiments were performed with an increasing shear rate (0.5–800 s^{-1}) using the continuous ramp procedure. The viscosity versus temperature data were collected using the constant share rate method (100 s^{-1}). In this measurement, the sample was quickly heated to 110 °C and equilibrated at that temperature for 5 min, then cooled at a constant rate (1.0 and 3.0 °C/min). Sampling points were recorded every 1 °C.

3. Results and Discussion

3.1. Functional Group Identification and Interaction

FT-IR analysis was conducted to identify the major functional groups in kernel fats and pulp oils, assess potential functional group interactions and compare characteristic wavebands and shifts between the pulp oils and kernel fats. This information can be used to help make informed decisions on formulating materials and mixtures that would be suitable for specialized foods and cosmetics. The FTIR spectra of the pulp oils (AVP and AAP oils) are similar, so are the FTIR spectra of the kernel fats (AVK and AAK fats). The FT-IR spectra of AAP oil and AAK fat are shown in Figure 2b–d and illustrate the differences between these oils and fats. The FT-IR spectra of the pulp oils and kernel fats of AV and AK are presented in Figure 2. The characteristic absorption bands and their assignments are presented in Table 1.

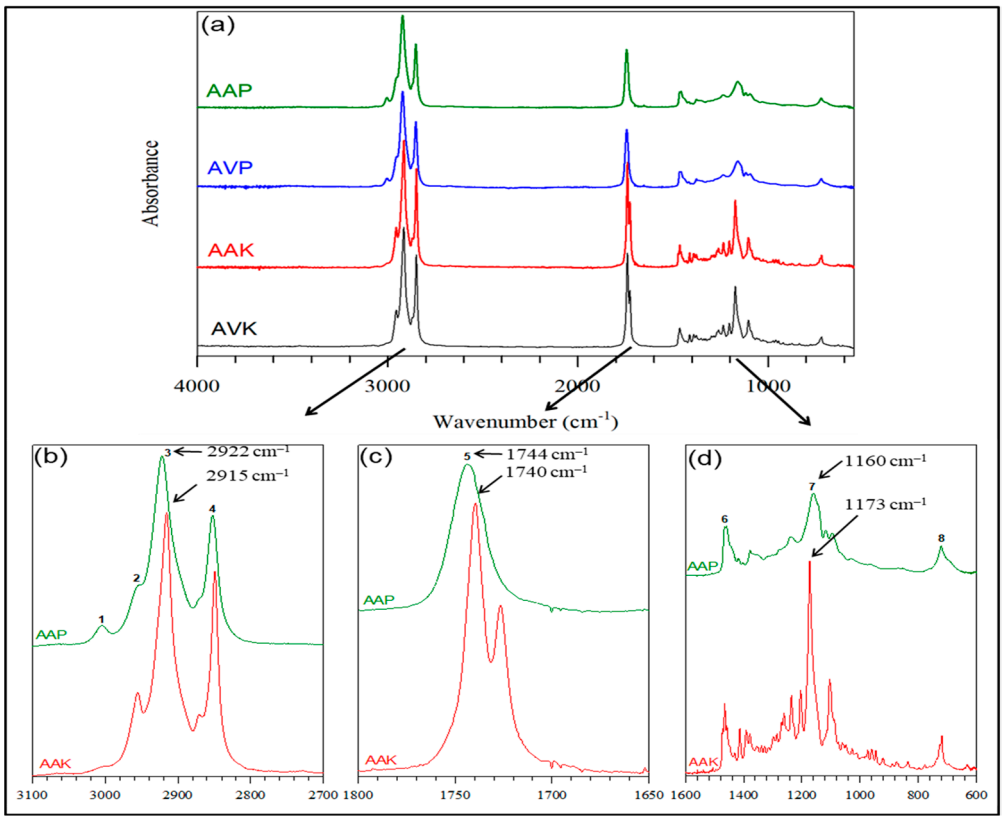

Figure 2. (**a**) FTIR spectra of *Astrocaryum vulgare* kernel (AVK) fat, *Astrocaryum aculeatum* kernel (AAK) fat, *Astrocaryum vulgare* pulp (AVP) oil and *Astrocaryum aculeatum* pulp (AAP) oil. (**b**–**d**) Zoom in of the characteristic (3100–2700) cm^{-1}, (1800–1650) cm^{-1} and (1600–600) cm^{-1} wave band regions, respectively, of AAK fat and AAP oil. Bands are labeled 1–8 from the highest to lowest wavenumber.

Table 1. FT-IR characteristic absorption bands for *Astrocaryum vulgare* and *Astrocaryum aculeatum* pulp oils and kernel fats.

Peak Number	Band Position (cm^{-1})	Wavelength (nm)	Assignment
1	3005	3328	*Cis* double-bond (H–C=C–H) *sym* stretch
2	2953	3386	Methyl group (C–H) *asym* stretch
3	2925	3419	Methylene group (C–H) *asym* stretch
4	2854	3504	Methyl and methylene group (C–H) *sym* stretch
5	1740	5747	Ester carbonyl group (C=O) stretch
6	1460	6849	Methylene ($C–H_2$) scissoring
7	1161	8613	Alkoxy group (C–O) stretch
8	722	13,850	Methylene group ($C–H_2$) rocking

FTIR (Figure 2) indicates that the pulp oils and kernel fats extracted from AV and AA fruits are predominantly composed of TAGs. The presence of TAG structures is confirmed by the presence of ester functional groups (peak 5, C=O stretch at 1740 cm^{-1} and peak 7, C–O stretch 1161 cm^{-1}, see Figure 2) and fatty chains (peak 2, methyl *asym* C–H stretch at 2953 cm^{-1}, peak 3, methylene C–H *asym* stretch at 2925 cm^{-1}, peak 4, and C–H *sym* stretch 2854 cm^{-1}). AAP and AVP oils presented similar FTIR profiles with similar wavenumbers and intensities, indicating similar molecular profiles. AAK and AVK fats also presented similar FTIR profiles, indicating similar molecular makeups. The differences between the pulp oils and kernel fats manifested in the stronger *cis* double-bond (H-C=C-H) *sym*

stretch (peak 1 at 3005 cm^{-1} in Figure 2) of the pulp oils compared to the kernel fats, indicating significant differences in the levels of unsaturated TAGs and the contribution from carotenoids [42], which is in agreement with previous observations. There are also notable differences in broadening between the absorption band peaks of pulp oils and kernel fats due to differences in translational and rotational molecular motion between the liquid and solid states. The absorption bands of the pulp oils are broader than those of the kernel fats (Figure 2b–d), particularly the carbonyl group (peak 5) and alkoxy group (peak 7) because of the much higher degree of freedom and increased molecular vibrations of AVP and AAP molecules in the liquid state compared to the AVK and AAK molecules in the solid state.

3.2. Lipid Composition

Tables 2–5 present the lipid components of AVP, AVK, AAP and AAK, respectively.

AVP oil is dominated by three categories of TAGs: two di-unsaturated TAGs, POO, with a relative intensity (RI) of 43.01%, and SOO (9.13%); one mono-unsaturated TAG (POP with an RI of 17.33%); and triolein (OOO, RI of 27%). The AVP oil was 65% unsaturated, with the constituent fatty acids entirely comprised of palmitic, stearic and oleic acids, with palmitic acid the most abundant saturated fatty acid. Similar results were reported by Santos et al. in 2013 [25], identifying POO as the major TAG in AVP extracted from fruits collected in the State of Amapa, Brazil. However, the result of this work differs from that of Oboh and Oderinde. in 1998 [23], where SOO was reported as the main TAG in AVP extracted from Nigerian fruits and no TAGs containing palmitic acid were observed.

Table 2. *Astrocaryum vulgare* pulp oil lipid compounds analyzed with a Thermo QExactive Orbitrap mass spectrometer in positive ionization mode. Compounds were detected as their Na^+ adducts, as predicted from their theoretical mass.

Compound	Abbr.	Chemical Formula	[M] (amu)	$[M+Na]^+$ (m/z)	Relative Intensity (%)
Triacylglycerols (TAGs)					
2-(palmitoyloxy)propane-1,3-diyl dioleate	POO	$C_{55}H_{102}O_6$	858.76	881.76	43.046
propane-1,2,3-triyl trioleate (OOO)	OOO	$C_{57}H_{104}O_7$	884.77	907.77	27.868
2-(oleoyloxy)propane-1,3-diyl dipalmitate	POP	$C_{53}H_{100}O_6$	832.75	855.74	17.333
2-(stearoyloxy)propane-1,3-diyl dioleate	SOO	$C_{57}H_{106}O_6$	886.80	909.78	9.131
3-(oleoyloxy)propane-1,2-diyl distearate	SSO	$C_{57}H_{108}O_6$	888.81	911.79	1.275
propane-1,2,3-triyl tristearate	SSS	$C_{57}H_{110}O_6$	890.83	913.75	0.822
propane-1,2,3-triyl tripalmitate	PPP	$C_{51}H_{98}O_6$	806.74	829.73	0.525
Diacylglycerols (DAGs)					
2-hydroxypropane-1,3-diyl dioleate	OO	$C_{39}H_{72}O_5$	620.54	643.53	51.993
3-hydroxy-2-(palmitoyloxy)propyl oleate	PO	$C_{39}H_{70}O_5$	594.52	617.51	42.326
2-hydroxypropane-1,3-diyl dipalmitate	PP	$C_{35}H_{68}O_5$	568.51	591.50	5.681
Monoacylglycerols (MAGs)					
2,3-dihydroxypropyl oleate	O	$C_{21}H_{40}O_4$	356.29	379.28	78.716
1,3-dihydroxypropan-2-yl palmitate	P	$C_{19}H_{38}O_4$	330.28	353.28	21.284

Table 3. *Astrocaryum vulgare* kernel fat lipid compounds analyzed with a Thermo QExactive Orbitrap mass spectrometer in positive ionization mode. Compounds were detected as their Na^+ adducts, as predicted from their theoretical mass.

Compound	Abbr.	Chemical Formula	[M] (amu)	$[M+Na]^+$ (*m*/*z*)	Relative Intensity (%)
Triacylglycerols (TAGs)					
propane-1,2,3-triyl tridodecanoate	LLL	$C_{39}H_{74}O_6$	638.55	661.54	30.07
3-(tetradecanoyloxy)propane-1,2-diyl didodecanoate	LLM	$C_{41}H_{78}O_6$	666.58	689.57	26.10
3-(dodecanoyloxy)propane-1,2-diyl ditetradecanoate	MML	$C_{43}H_{82}O_6$	694.61	717.60	9.99
3-(decanoyloxy)propane-1,2-diyl didodecanoate	LLC_{10}	$C_{37}H_{70}O_6$	610.52	633.51	11.97
3-(octanoyloxy)propane-1,2-diyl didodecanoate	LLC_8	$C_{35}H_{66}O_6$	582.49	605.48	10.49
3-(tetradecanoyloxy)propane-1,2-diyl didodecanoate	MMM	$C_{45}H_{86}O_6$	722.64	745.64	3.06
3-(oleoyloxy)propane-1,2-diyl didodecanoate	LLO	$C_{45}H_{84}O_6$	720.63	743.62	1.31
3-(hexanoyloxy)propane-1,2-diyl didodecanoate	LLC_6	$C_{33}H_{62}O_6$	554.45	577.44	2.21
1-(dodecanoyloxy)-3-(tetradecanoyloxy)propan-2-yl oleate	LOM	$C_{47}H_{88}O_6$	748.66	771.65	0.94
2-(dodecanoyloxy)propane-1,3-diyl dioleate	LOO	$C_{51}H_{94}O_6$	802.71	825.69	0.79
3-(palmitoyloxy)propane-1,2-diyl ditetradecanoate	MMP	$C_{47}H_{90}O_6$	750.67	773.66	0.93
3-(oleoyloxy)propane-1,2-diyl ditetradecanoate	MMO	$C_{49}H_{92}O_6$	776.69	799.69	0.00
2-(tetradecanoyloxy)propane-1,3-diyl dioleate	MOO	$C_{53}H_{96}O_6$	830.74	853.72	0.32
3-(dodecanoyloxy)-2-(tetradecanoyloxy)propyl (9Z,12Z)-octadeca-9,12-dienoate	LLiM	$C_{47}H_{88}O_6$	745.64	769.62	0.47
propane-1,2,3-triyl trioleate	OOO	$C_{57}H_{104}O_7$	884.77	907.77	0.35
2-(palmitoyloxy)propane-1,3-diyl dioleate	POO	$C_{55}H_{102}O_6$	858.76	881.76	0.27
3-(((9Z,12Z)-octadeca-9,12-dienoyl)oxy)propane-1,2-diyl didodecanoate	LLLi	$C_{45}H_{82}O_6$	718.61	741.59	0.39
2-(dodecanoyloxy)propane-1,3-diyl dioctanoate	LC_8C_8	$C_{31}H_{58}O_6$	526.42	549.42	0.34
Diacylglycerols (DAGs):					
2-hydroxy-3 (tetradecanoyloxy)propyl palmitate	PM	$C_{33}H_{64}O_5$	540.48	563.38	22.48
3-hydroxypropane-1,2-diyl didodecanoate	LL	$C_{27}H_{52}O_5$	456.38	479.37	54.37
3-(dodecanoyloxy)-2-hydroxypropyl tetradecanoate	LM	$C_{29}H_{56}O_5$	484.41	507.37	19.95
3-hydroxypropane-1,2-diyl ditetradecanoate	MM	$C_{31}H_{60}O_5$	512.44	535.44	3.21
Monoacylglycerols (MAGs)					
1,3-dihydroxypropan-2-yl palmitate	P	$C_{19}H_{38}O_4$	330.28	353.26	100

AAP oil, despite the similarity to AVP oil in genus, fruit taxonomy, oil appearance and other measured macrofunctionalities, demonstrated unexpected differences in its TAG profile, as well as unsaturation levels and fatty acid diversity. AAP oil was dominated by two classes of TAGs: tri-unsaturated TAGs, OOO (RI of 38.04%), OOLi (RI = 16.99%), OLiLi (RI = 8.65%) and LiLiLi (RI of 2.34%) and di-unsaturated TAGs, SOO (RI of 18.72%) and POO (RI of 13.49%). The AAP oil was 80% unsaturated, with constituent fatty acids of the palmitic, stearic, oleic and linoleic varieties and stearic acid as the most abundant saturated fatty acid.

Table 4. *Astrocaryum aculeatum* pulp oil lipid compounds analyzed with a Thermo QExactive Orbitrap mass spectrometer in positive ionization mode. Compounds were detected as their Na^+ adducts, as predicted from their theoretical mass.

Compound	Abbr.	Chemical Formula	[M] (amu)	$[M+Na]^+$ (*m*/*z*)	Relative Intensity (%)
Triacylglycerols (TAGs)					
propane-1,2,3-triyl trioleate	OOO	$C_{57}H_{104}O_6$	884.77	907.77	38.04
2-(stearoyloxy)propane-1,3-diyl dioleate	SOO	$C_{57}H_{106}O_6$	886.80	909.78	18.72
3-(((9Z,12Z)-octadeca-9,12-dienoyl)oxy)propane-1,2-diyl dioleate	OOLi	$C_{57}H_{102}O_6$	882.77	905.75	16.99
2-(palmitoyloxy)propane-1,3-diyl dioleate	POO	$C_{55}H_{102}O_6$	858.76	881.76	13.49
2-(oleoyloxy)propane-1,3-diyl (9Z,9′Z,12Z,12′Z)-bis(octadeca-9,12-dienoate)	OLiLi	$C_{57}H_{100}O_6$	880.75	903.74	8.65
propane-1,2,3-triyl tri[(9Z,12Z)-octadeca-9,12-dienoate]	LiLiLi	$C_{57}H_{98}O_6$	878.74	901.74	2.34
2-(oleoyloxy)propane-1,3-diyl dipalmitate	PPO	$C_{53}H_{100}O_6$	832.75	855.74	1.76
Diacylglycerols (DAGs)					
2-hydroxypropane-1,3-diyl dioleate	OO	$C_{39}H_{72}O_5$	620.54	643.53	78.55
3-hydroxy-2-(palmitoyloxy)propyl oleate	PO	$C_{39}H_{70}O_5$	594.52	617.51	19.90
2-hydroxypropane-1,3-diyl dipalmitate	PP	$C_{35}H_{68}O_5$	568.51	591.50	1.55
Monoacylglycerols (MAGs)					
2,3-dihydroxypropyl oleate	O	$C_{21}H_{40}O_4$	356.29	379.29	77.82
1,3-dihydroxypropan-2-yl palmitate	P	$C_{19}H_{38}O_4$	330.28	353.28	22.18

Based on the relative intensities, the di-unsaturated TAG POO is the major TAG in AVP oil, whereas the tri-unsaturated OOO is the major TAG in AAP oil. Although both pulp oils are largely composed of unsaturated TAGs, the highly unsaturated AAP oil contained no tri-saturated TAGs and only a small amount of di-saturated TAGs (PPO at a RI of 1.34%). AVP oil contains a small amount of both tri-stearin and tri-palmitin (combined RI of 3%), as well as SSO (RI of 1.27%). From a crystallization perspective, it is therefore expected that the relatively higher percentages of tri- and di-saturated TAGs that exist in AVP oil should lead to earlier nucleation at similar undercooling levels. Of particular interest, AV proliferates on flat marine-rich alluvial coastal plains and lowlands close to the coast, whereas AA proliferates in dense rainforest highlands further inland, which have ferrous and low-organic-matter-content soils and relatively cooler daily average temperatures. From the comparison of their saturates, AVP is a palmitic-rich oil, whereas AAP is a stearic-rich oil. Furthermore, it was expected that AAP oil would be significantly more susceptible to oxidative rancidity due to its higher levels of oleic acid and the significant presence of linoleic acid (10 times more susceptible to oxidative cleavage than oleic acid). The significantly higher unsaturation of AAP oils, together with the presence of the ω-6 essential fatty acid linoleic acid, suggests that it is a healthier edible oil compared to AVP oil but is significantly more susceptible to oxidative degradation and deteriorating quality. Although it has been reported that the pulp oils contain ω-3, ω-6 and ω-9 fatty acids [21,24], the analysis of the pulp oils sourced from Guyana showed that they contained only ω-9 fatty acids in the case of AVP oil and only ω-6 and ω-9 fatty acids in the AAP oil.

Table 5. *Astrocaryum aculeatum* kernel fat lipid compounds analyzed with a Thermo QExactive Orbitrap mass spectrometer in positive ionization mode. Compounds were detected as their Na^+ adducts, as predicted from their theoretical mass.

Compound	Abbr.	Chemical Formula	[M] (amu)	$[M+Na]^+$ (*m*/*z*)	Relative Intensity (%)
Triacylglycerols (TAGs)					
propane-1,2,3-triyl tridodecanoate	LLL	$C_{39}H_{74}O_6$	638.55	661.54	30.90
3-(tetradecanoyloxy)propane-1,2-diyl didodecanoate	LLM	$C_{41}H_{78}O_6$	666.58	689.57	26.08
3-(dodecanoyloxy)propane-1,2-diyl ditetradecanoate	MML	$C_{43}H_{82}O_6$	694.61	717.60	10.46
3-(decanoyloxy)propane-1,2-diyl didodecanoate	LLC_{10}	$C_{37}H_{70}O_6$	610.52	633.51	8.98
3-(octanoyloxy)propane-1,2-diyl didodecanoate	LLC_8	$C_{35}H_{66}O_6$	582.49	605.48	7.43
propane-1,2,3-triyl tritetradecanoate	MMM	$C_{45}H_{86}O_6$	722.64	745.64	3.69
3-(oleoyloxy)propane-1,2-diyl didodecanoate	LLO	$C_{45}H_{84}O_6$	720.63	743.62	2.37
3-(hexanoyloxy)propane-1,2-diyl didodecanoate	LLC_6	$C_{33}H_{62}O_6$	554.45	577.44	1.87
1-(dodecanoyloxy)-3-(tetradecanoyloxy)propan-2-yl oleate	LOM	$C_{47}H_{88}O_6$	748.66	771.65	1.73
3-(dodecanoyloxy)propane-1,2-diyl dioleate	LOO	$C_{51}H_{94}O_6$	802.71	825.69	1.49
3-(palmitoyloxy)propane-1,2-diyl ditetradecanoate	MMP	$C_{47}H_{90}O_6$	750.67	773.66	1.23
3-(oleoyloxy)propane-1,2-diyl ditetradecanoate	MMO	$C_{49}H_{92}O_6$	776.69	799.69	1.12
3-(dodecanoyloxy)-2-(tetradecanoyloxy)propyl (9Z,12Z)-octadeca-9,12-dienoate	LLiM	$C_{47}H_{88}O_6$	745.64	769.62	0.53
propane-1,2,3-triyl trioleate	OOO	$C_{57}H_{104}O_7$	884.77	907.77	0.52
3-(((9Z,12Z)-octadeca-9,12-dienoyl)oxy)propane-1,2-diyl didodecanoate	LLLi	$C_{45}H_{82}O_6$	718.61	741.59	0.34
2-(tetradecanoyloxy)propane-1,3-diyl dioleate	MOO	$C_{53}H_{96}O_6$	830.74	853.72	0.59
2-(palmitoyloxy)propane-1,3-diyl dioleate	POO	$C_{55}H_{102}O_6$	858.76	881.76	0.38
2-(dodecanoyloxy)propane-1,3-diyl dioctanoate	LC_8C_8	$C_{31}H_{58}O_6$	526.42	549.42	0.29
Diacylglycerols (DAGs)					
3-hydroxypropane-1,2-diyl didodecanoate	LL	$C_{27}H_{52}O_5$	456.38	479.37	58.10
3-(dodecanoyloxy)-2-hydroxypropyl tetradecanoate	LM	$C_{29}H_{56}O_5$	484.41	507.37	37.58
3-hydroxypropane-1,2-diyl ditetradecanoate	MM	$C_{31}H_{60}O_5$	512.44	535.44	4.32
Monoacylglycerols (MAGs)					
1,3-dihydroxypropan-2-yl palmitate	P	$C_{19}H_{38}O_4$	330.28	353.26	100

AVK and AAK fats are compositionally very similar, despite the significant compositional differences in the corresponding pulp oils. Both kernel fats are 80% saturated with five major tri-saturated TAGs: LLC_8, LLC_{10}, LLL, MML and LLM. Of these, trilaurin and LLM predominate. The predominating saturated fatty acids are lauric, myristic, capric and caprylic acids, with small amounts of caproic and palmitic acids (the acids are listed in descending relative intensities in the foregoing list). Oleic acid is the predominating unsaturated fatty acid, with trace amounts of linoleic acid. Interestingly, neither of the kernel fats contained stearic acid.

The pulp oils contain no medium-chain fatty acids, whereas the kernel oils are mostly composed of medium-chain fatty acids. The kernel oils are similar in this way to coconut oil and palm kernel oil and may provide a valuable source of MCTs if the myristic acid content can be removed through fractionation or other means. MCTs are important nutritionally, pharmaceutically and cosmetically [43].

3.3. Thermal Degradation

Figure 3a,b presents the TGA and DTG curves for the AAP and AVP oils and the AAK and AVK fats. The tabulated TGA data, with onset of mass loss ($T_{5\%}^{ON}$) and maximum mass loss (T_D), are presented in Table 6. Ash percentages in all samples were <0.1%, confirming the complete degradation and volatilization of these fats and oils.

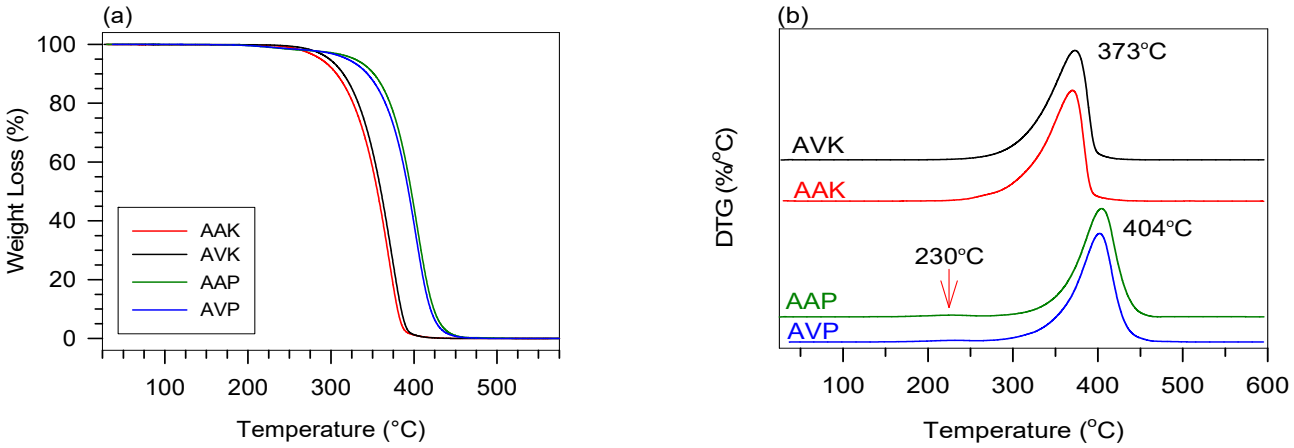

Figure 3. (**a**) TGA and (**b**) DTG curves of *Astrocaryum vulgare* kernel (AVK) fat, *Astrocaryum aculeatum* kernel (AAK) fat, *Astrocaryum vulgare* pulp (AVP) oil and *Astrocaryum aculeatum* pulp (AAP) oil. DTG peak values are reported on the curves of panel (**b**).

Table 6. Tabulated TGA onset of mass loss ($T_{5\%}^{ON}$) and maximum mass loss (T_D). The standard deviation is ±2 °C for the temperatures, n = 2.

Samples	TGA	DTG	
	$T_{5\%}^{ON}$ (°C)	T_{D1} (°C)	T_{D2} (°C)
AAK	287	370	-
AVK	298	373	-
AAP	329	405	233
AVP	320	402	231

The DTG curves are characteristic of a mass loss dominated by evaporation [44]. As shown in Table 6, the pulp oils exhibit the onset of mass loss $\left(T_{5\%}^{ON}\right)$ 31 ± 9 °C higher than the kernel fats. These variations in $T_{5\%}^{ON}$ are likely due to differences in their lipid composition. The pulp oils primarily consist of unsaturated TAGs comprised of long-chain C16 and C18 fatty acids, whereas the kernel fats are predominantly composed of saturated TAGs containing short- and medium-chain C6-C14 fatty acids, with a predominance of C12. The rate of evaporation is influenced by the molecular mass (m) of compounds. The major TAGs in the kernel fats, comprising of short- and medium-chain fatty acids, are approximately 24% lower in molecular mass compared to the TAGs present in the pulp oils, likely resulting in their evaporation at lower temperatures relative to the pulp oils. The differences in $T_{5\%}^{ON}$ are also evident between the pulp oils, with the $T_{5\%}^{ON}$ of AAP oil being 9 ± 1 °C higher than that of AVP oil. Despite AAP being significantly more unsaturated, it contains significantly more C18 fatty acids than C16 fatty acids, which explains the higher evaporation onset temperature (higher molecular masses). For example, the molecular mass of triolein is 885.43 g/mol, compared to 859.40 g/mol for POO, with POO being the most abundant TAG in AVP oil and OOO being the most abundant TAG in AAP oil. Comparing the AV and AA kernel fats, the $T_{5\%}^{ON}$ of AVK is 11 ± 1 °C higher than that of AAK. AAK has a higher abundance of low molecular mass, short-chain TAGs (e.g., LLC_{10} and LLC_8), likely the reason for the lower $T_{5\%}^{ON}$ compared to AVK.

3.4. Thermal Phase Behavior

The cooling (5 °C/min) and heating (10 °C/min) DSC thermograms of *Astrocaryum vulgare* and *Astrocaryum aculeatum* oils and fats are presented in Figure 4a,b, respectively. The corresponding crystallization and melting data are provided in Table 7.

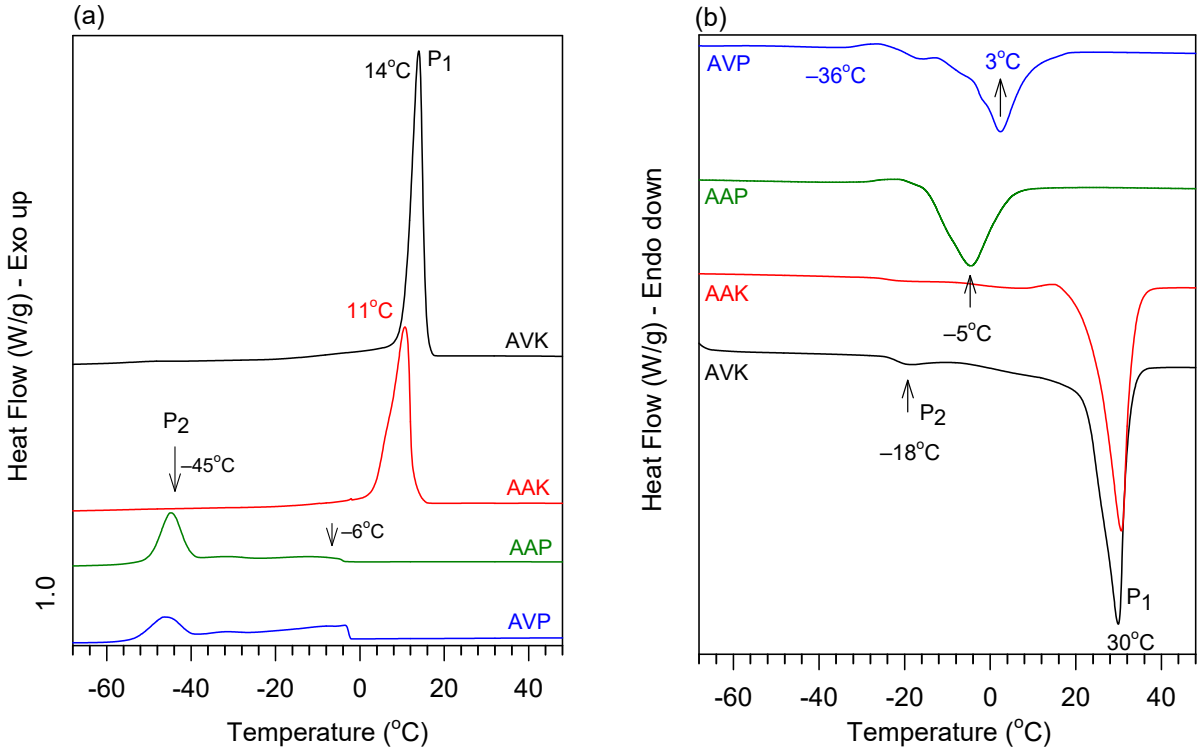

Figure 4. (**a**) Cooling (5 °C/min) and (**b**) heating (10 °C/min) DSC thermograms of *Astrocaryum vulgare* kernel (AVK) fat, *Astrocaryum aculeatum* kernel (AAK) fat, *Astrocaryum vulgare* pulp (AVP) oil and *Astrocaryum aculeatum* pulp (AAP) oil.

Table 7. Crystallization and melting data for *Astrocaryum vulgare* and *Astrocaryum aculeatum* pulp (AVP and AAP) oils and kernel (AVK and AAK) fats. The standard deviation is ±1 °C for the temperature and ±5 J/g for enthalpy, $n = 2$.

Sample	T_{ON} **(°C)**	T_{C1} **(°C)**	T_{C2} **(°C)**	T_{C3} **(°C)**	T_{OFF} **(°C)**	ΔH_{total} **(J/g)**
			Crystallization			
AAK	12	11	--	--	3	123
AVK	16	14	--	--	10	130
AVP	−2	−5	−32	−46	−54	68
AAP	1	−2	−31	−45	−51	62
			Melting			
Sample	T_{ON} **(°C)**	T_{m1} **(°C)**	T_{m2} **(°C)**	T_{m3} **(°C)**	T_{OFF} **(°C)**	ΔH_{total} **(J/g)**
AAK	−27	−18	31	--	34	125
AVK	−29	−19	30	--	33	133
AVP	−53	−35	−16	3	11	76
AAP	−59	−43	−5	--	4	67

3.4.1. Crystallization

The cooling thermograms of the kernel fats are characterized by sharp events (T_{C1}) at 11 °C for AAK and 14 °C for AVK and are similar to the crystallization behavior of the lauric-rich systems observed by Bouzidi et al. [45] and Macridachis et al. [46].

AVP and AAP pulp oils presented only subzero exothermic events, with a leading broad event and an extended small event peaking at -5 ± 1 °C and -2 ± 1 °C, respectively, followed by a distinct low-intensity broad event for both pulp oils at -32 ± 1 °C and an intense well-resolved exotherm for both pulp oils at -45 ± 1 °C. These exotherms could be related to three different groups, each comprising TAGs with similar unsaturation levels and stereospecificities.

The tri-saturated and di-saturated TAGs, such as PPP, SSS, SSO and PPO, are expected to be the initial group to crystallize (at $\boldsymbol{T_{C1}}$). The peak observed at $\boldsymbol{T_{C1}}$ represents <5% of the overall enthalpy of crystallization, likely owing to the low abundance of these TAGs in the pulp oils.

Unsaturated TAGs, with the kinks introduced by double bonds, exhibit lower crystallization temperatures, as their disrupted molecular packing results in weaker intermolecular forces. The peaks observed at $\boldsymbol{T_{C2}}$ represent approximately 16% of the total enthalpy of crystallization for both pulp oils and are more likely associated with di-unsaturated TAGs such as POO and SOO.

The lowest exotherms ($\boldsymbol{T_{C3}}$) for AVP and AAP at -48 ± 2 °C distinctly separate from the others, likely related to the partial crystallization of OOO. The exotherms ($\boldsymbol{T_{C3}}$) for AVP and AAP in this work are similar to those observed by Nagamizu et al. [47] for pure OOO, which was characterized by a broad, symmetrical peak from approximately -30 °C to -40 °C. The enthalpy of crystallization at $\boldsymbol{T_{C3}}$ for AVP is 47% less than that observed for AAP, potentially attributed to the abundance of OOO in AVP being approximately 36% lower than that in AAP.

3.4.2. Melting

The melting ranges, as observed from Figure 4 and Table 7, generally do not coincide with the crystallization ranges for fats and oils because of the undercooling and kinetic effects and melt-mediated crystal ripening [48–50].

Both kernel fats exhibited distinct melting thermograms marked by sharp exotherms at 30 °C. The similarity in their melting ranges is due to their remarkably similar lipid compositions. A low-intensity exotherm is observed at -18.5 ± 1 °C for both kernel fats, likely due to low melting components with low relative abundances, such as LOO, MOO and POO.

The pulp oils presented more complex melting behavior characterized by low-intensity peaks (T_{m1}) at -35 °C and -43 °C for AVP and AAP, respectively, likely corresponding to tri-unsaturated and di-unsaturated TAGs (e.g., OOO and POO). AVP oil presented a shoulder peak at -16 °C that was not present in AAP and was possibly associated monounsaturated TAGs (e.g SSO and LOS) that were not present in AAP.

The main exothermic events (T_{m3}) are at 3 ± 1 °C and -5 ± 1 °C for the AVP and AAP pulp oils, respectively. The higher melting temperature at T_{m3} for AVP is clearly a result of the higher level of saturation, as well as the nucleating and crystal growth propensity of the TAGs, such as SSS, PPP, POP and SSO (relative abundances of 2, 1, 40 and 3%, respectively), present in AVP oil compared to the absence of tri-saturates and the only 5% relative abundance of di-saturates in AAP oil.

3.5. Crystal Type and Polymorphism

XRD scans of the AAP and AVP oils did not present any crystal peaks, confirming the DSC data that indicated that these oils are liquid at room temperature. The WAXD and SAXD spectra obtained for AAK and AVK fats are shown in Figure 5. The d-spacings and related Miller indices of their WAXD and SAXD are provided in the Supplementary Materials Table S1.

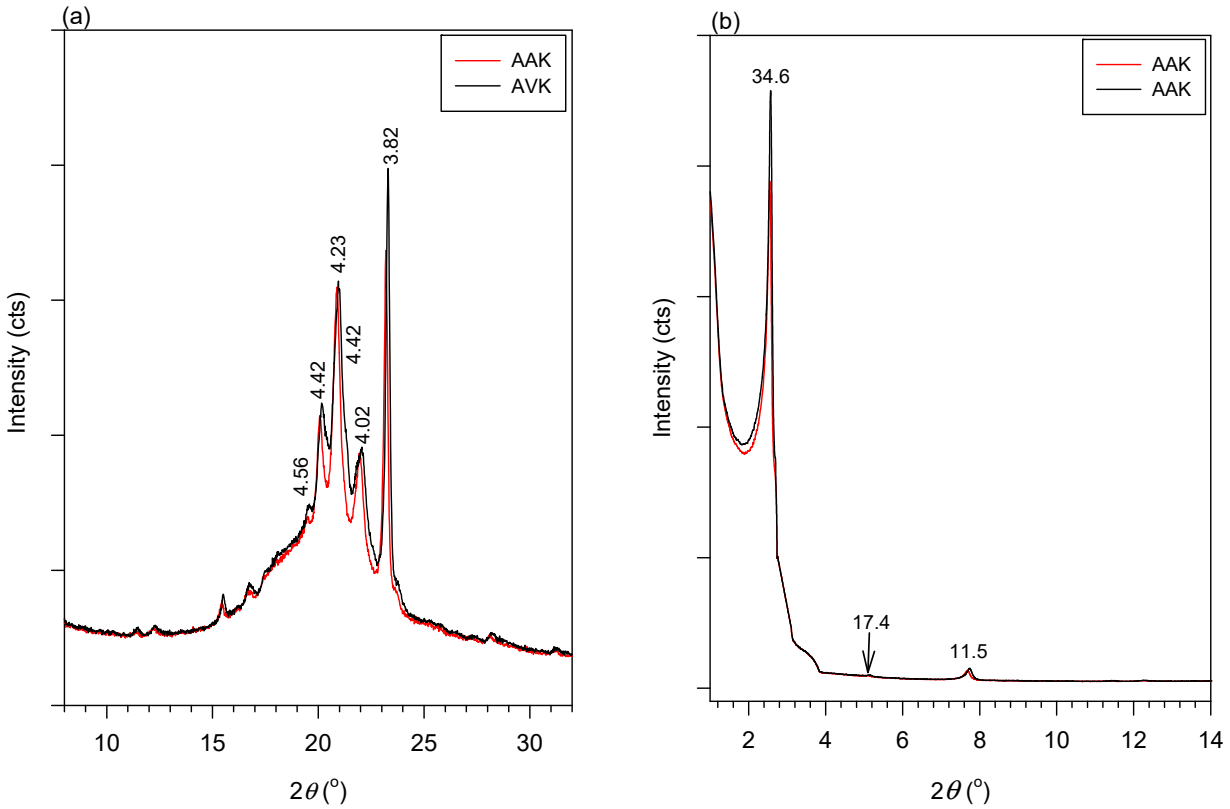

Figure 5. (**a**) Small-angle X-ray diffraction (SAXD) and (**b**) wide-angle X-ray diffraction (WAXD) of *Astrocaryum aculeatum* (AAK) and *Astrocaryum vulgare* (AVK) fats measured at room temperature.

As can be seen in Figure 5, the AAK and AVK fats show similar XRD peaks, indicating similar crystal phases. The WAXD crystal peaks of both the AVK and AAK fats are superimposed to a wide background halo that was fitted at approximately 4.8 Å, indicating the presence of liquid phases. The crystallinity, as determined by the crystal peaks area to total area, is 81% for AAK and 78% for AVK. These melting points of the crystalline phase occurred at 30 °C, with enthalpies in the range of 125–130 J/g.

WAXD of the AVK and AAK fats indicates a large percentage of the crystalline packing is in the β'-packing arrangement (prominent diffraction peaks at 4.2 Å (110) and 3.8 Å (200), characteristic of the β'-orthorhombic subcell structure) and a small percentage of the crystals are arranged in the β-packing arrangement, as indicated by low-intensity reflections at 4.6 Å, 3.8 Å and 3.6Å, characteristic of a triclinic parallel subcell [51]. The reflection at 3.8 Å is common to β' and β subcells. Its high intensity is the result of the combined contributions from the β' and β' structures. In both fats, the β-phase content estimated from the main characteristic peaks is less than 10% of the entire crystalline phase. The ability of fats to crystallize in the beta prime (β') form is important for producing products with a smooth texture, such as margarine and some cosmetics. Further research on how to achieve this crystallization more consistently would potentially help in achieving the desired texture and stability in food and cosmetic formulations with these products. The cross-sectional packing of AAK and AVK fats in the orthorhombic subcell (β') and triclinic subcell (β) are shown in a and b, respectively.

The 001 SAXD reflections of AVK and AAK fats indicate that the molecules have a stacking length of 35 Å along the c-axis (d_{001} = 35 Å, d_{002} = 17.4 Å and d_{003} = 11.5 Å, Figure 6). This 35 Å experimental stacking length is consistent with double chain length (DCL) stacking of two trilaurin molecules oriented in the chair configuration (see Figure 6).

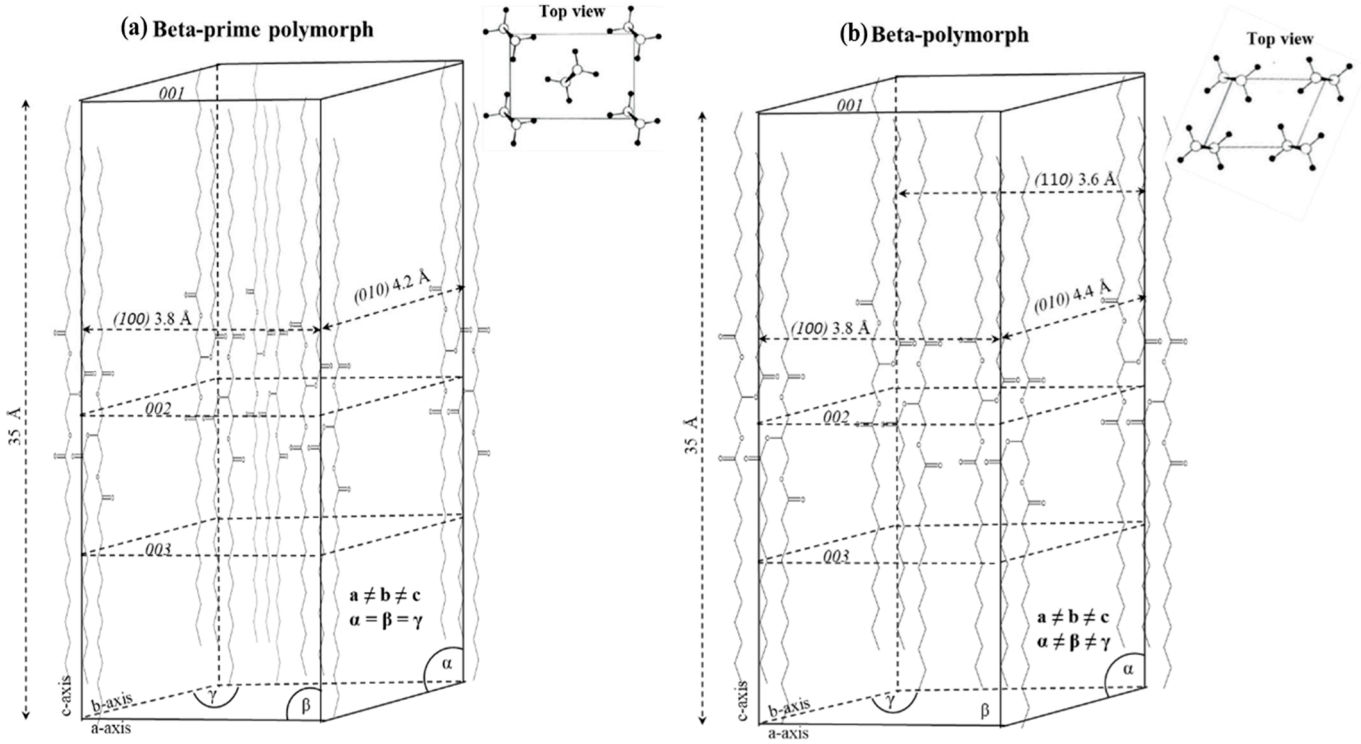

Figure 6. Schematic representation of the cross-sectional packing of the kernel fats (**a**) in orthorhombic subcell (β') and (**b**) in triclinic subcell (β). Inset shows the methyl-end top-view projection of the unit cells.

3.6. Microstructure

Figure 7 presents the micrographs of AVP, AAP, AVK and AAK. Images were captured at the main crystallization temperature under 50×, 100× and 500× magnifications.

From Figure 7, both AVP and AAP pulp oil have rod-shaped crystals at −45 °C. However, crystallized AVP oil is characterized by crisply defined rods and significantly more centers of growth, suggesting a larger number of nuclei. This is of course supported by the higher saturation levels of AVP oil, as discussed earlier, and the increased presence of tri-saturated and di-saturated TAG species in AVP compared to the no tri-saturated TAGS and the very low content of di-saturated TAGs in AAP. The crystallized forms of these oils are likely to be rarely encountered, as it is unlikely that they will ever see use in environments below −45 °C.

AVK and AAK fats demonstrate microstructures similar to cocoa butter, coconut oil and palm kernel oil in that they have a typically fractal self-similar structural organization [52]. Lipids with strong influence from lauric acid are known to form spherulitic-type structures that grow from the self-association of smaller centers of crystallization [53,54]. The individual centers of growth self-organize into self-similar structures at different length scales, as supported by the micrographs in Figure 7. The centers of growth at the larger length scales for AAK are approximately 50 to 100 times larger than those of AVK. It is still not understood why this is the case, although it is likely that the higher preponderance of short-chain fatty acids (C6 and C8) in AAK results in a significantly different growth mode, as detailed by Bouzidi and Narine [48]. It is expected that the shorter-chain fatty acids will result in asymmetrical TAGs that result in a raising of the activation energy for the diffusion of such TAGs in a configuration required for the participation in the growth of a crystal to the crystal's surface. This can, in turn, limit the centers of growth, resulting in larger spherulites. Given that both kernel fats achieve similar degrees of crystallization, the influence of the shorter-chain fatty acids in modifying the growth mode is an interesting phenomenon that can be exploited to modify the microstructure and texture of these fats through the processing conditions and interesterification.

A consequence of the microstructural organization of the kernel fats is that they are likely to provide brittle fats with excellent surface sheen and good de-molding properties, similar to cocoa butter and palm kernel oil. Furthermore, the AAK crystallized networks are likely to have a "softer" texture compared to AVK, given the closer packing of AVK and its increased number of centers of growth.

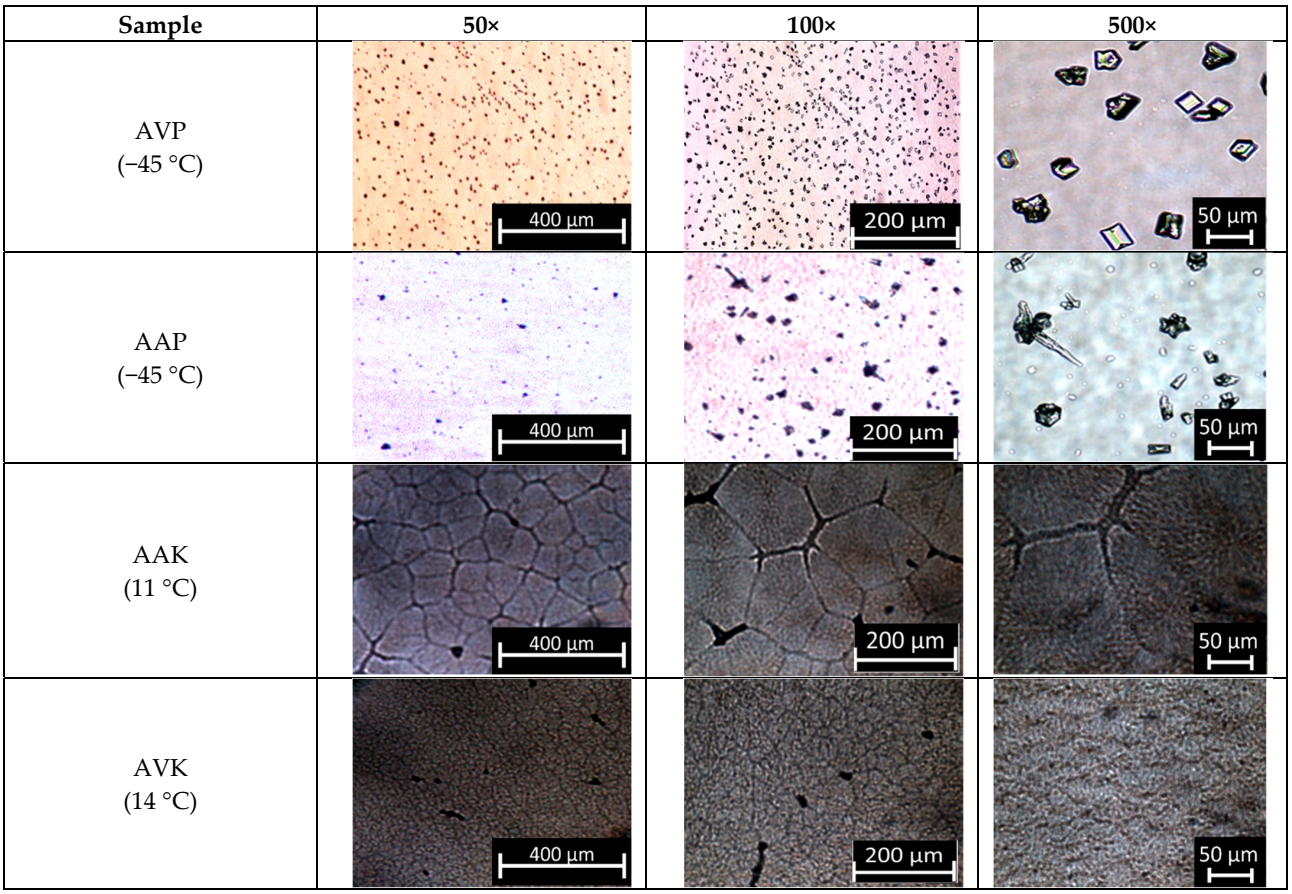

Figure 7. PLM images for AVK, AAK, AVP and AAP obtained at the main crystallization temperature under different magnifications when cooled at 5 °C/min.

3.7. Viscosity and Flow Behavior

Shear rate–shear stress curves and dynamic viscosity versus temperature curves are presented in Figure 8a,b, respectively. The corresponding rheological data are provided in the Supplementary Materials Tables S2 and S3, respectively.

The shear rate–shear stress curves were fitted with the Herschel–Bulkley equation (Equation (1)), a model commonly used to describe the general behavior of materials characterized by yield stress. A fit of the Newtonian model to the data did not provide any differences from the Herschel–Bulkley model.

$$\tau = \tau_0 + \kappa\gamma^n \quad (1)$$

τ: shear stress, γ: shear rate, τ_0: the yield stress below which there is no flow, k: consistency index and n: flow index. n depends on the constitutive properties of the material. For Newtonian fluids, $n = 1$ and $k = \eta$ is the fluid viscosity. For shear-thickening fluids, $n > 1$; for shear-thinning fluids, $n < 1$.

All pulp oils and kernel fats presented shear stress–shear rate curves that, when fitted to the Herschel–Bulkley model (Equation (1), $R^2 \geq 0.9999$), yielded a power index of $n = 1.000 \pm 0.001$ and stress values of less than 0.02 ± 0.02 Pa·s, indicating Newtonian flow behaviors Figure 8a).

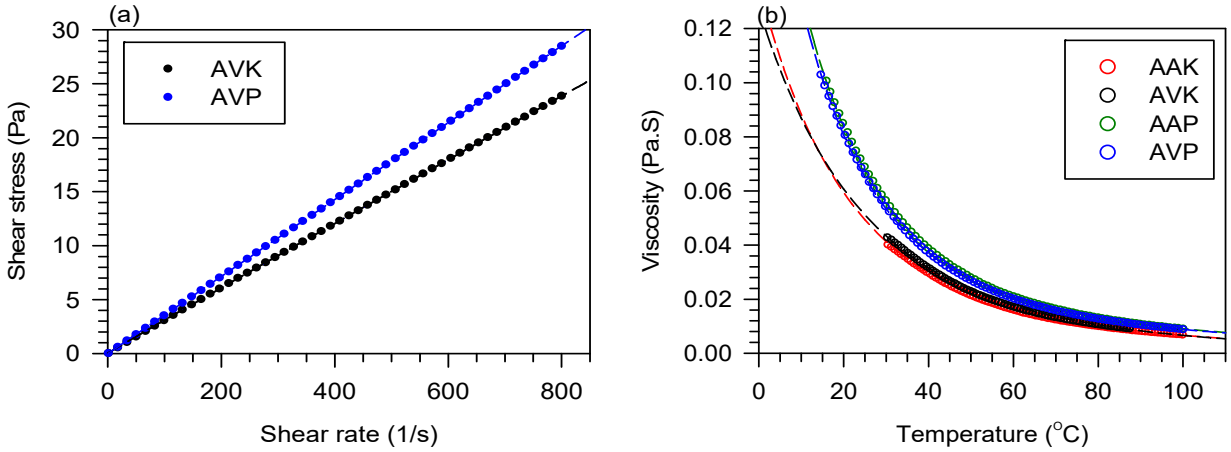

Figure 8. (**a**) Shear rate–shear stress curves at 40 °C and (**b**) dynamic viscosity versus temperature curves of AVK and AVP. Dashed lines are fits of the generalized van Velzen equation (Equation (2)) to the experimental data.

Figure 8b shows that all pulp oil and kernel fat viscosities decrease with temperature, following a typical exponential trend. Moreover, for any given temperature, the viscosity of the AAK and AVK were higher than that of the AAP and AVP (Figure 8b). This is most likely due to the higher degree of molecular organization possible in the melting of the medium-chain saturated fatty acid TAGs compared to the highly unsaturated pulp oils. The kernel fats (AAK and AVK) recorded almost identical viscosity temperature curves, as did the pulp oils (AAP and AVP).

The viscosity versus temperature data for the pulp oils and kernel fats were fitted with the generalized van Velzen equation (GvVE in Equation (2)) (Figure 8b).

$$ln(v) = A(-1 + \frac{1}{T^m}) \quad (2)$$

This model was selected from among several models available for predicting the viscosity of pure components and mixtures that are well documented in the literature. The model is a generalized version of the simple van Velzen equation and its closely related Andrade and generalized Andrade equations. The generalized forms are preferred because the number of fitting parameters is reduced and they are physically meaningful and quantifiably related to the magnitude of the viscosity and complexity of the pulp oils and kernel fats.

The GvVE model provided good fits for the viscosity versus temperature data for all pulp oils and kernel fats, regardless of the details of the molecular structure in the oil mixture. The fits were excellent, with determination coefficients $R^2 > 0.99$. The results of the fits (parameters A and exponent m) are provided in Table 8.

The GvVE fits yield physically meaningful parameters: parameter **A** relates directly to the magnitude of the viscosity of the liquid and exponent **m** relates to the complexity of the molecule. Table 8 shows that the AVP and AAP oils have similar viscosity magnitudes and complexities. Likewise, the AVK and AAK fats have similar viscosity magnitudes and complexities.

The viscosity differences between pulp oil and kernel fat can significantly influence their practical uses, especially in cosmetic formulations. The kernel fats, which remain solid at room temperature, serve well as thickening agents, contributing to the desired texture of products. In contrast, the more fluid pulp oils are capable of flowing at room temperature and are excellent for thinning cosmetic formulations. This distinction allows for the tailored use of each oil type, optimizing the textural and rheological properties of cosmetic products.

Table 8. Fit parameters for viscosity vs. temperature fittings using the generalized van Velzen model.

Samples	A	Std. Error	m	Std. Error
AVP	3.37	0.02	3.17	0.02
AAP	3.58	0.02	2.99	0.02
AVK	13.84	4.45	0.70	0.23
AAK	11.59	2.90	0.83	0.22

3.8. Comparison of the Chemical and Physical Properties with Other Selected Oils and Fats

The present materials can be appropriately compared to established lipids such as palm and coconut oils and shea and cocoa butters, as well as well-known tropical seed oils such as *Carapa guianensis* oil, commonly known as crabwood oil in Guyana and andiroba oil in Brazil, for potential suitability as ingredients in the food, cosmetics and pharmaceutical industries. Palm and coconut oils and shea and cocoa butters are versatile lipid materials and established liquid or fat systems that may be considered as models for comparison. Their solid fat content range and liquid properties allow an appropriate phase behavior comparison with the kernel fats and pulp oils of AV and AA. *Carapa guianensis* is an Amazonian oil that is currently actively studied and has demonstrated medicinal and cosmetic properties that highlights the possible added value uses of the present forest oils and fats for potential use in diverse food, cosmetic and pharmaceutical applications.

3.8.1. TAG Profile Comparison

Table 9 compares the TAG composition of AV and AA pulp oils and kernel fats with those of palm oil, shea butter, cocoa butter, *Carapa guianensis* oil and coconut oil. This TAG comparison was performed to gain insights into the possibilities of using AVP and AAP oils and AVK and AAK fats to mimic other oils and fats to attain a comparable outcome in functional properties. Such properties can help achieve desired textures, consistencies, processing and formulation and compatibility in recipes.

Table 9. Comparison of the TAG profiles of AV and AA pulp oils and kernel fats with selected oils and fats from the literature (shea butter [55], cocoa butter [56], palm oil [57], crude crabwood oil [58,59] and virgin coconut oil [60,61]). TAGs are presented in columns with descending relative intensities.

AVP (This Work)	AAP (This Work)	AVK (This Work)	AAK (This Work)	Palm Oil [57]	Shea Butter [55]	Cocoa Butter [56]	Crabwood Oil [58,59]	Coconut Oil [60,61]
POO 43.0%	OOO 38.0%	LLL 30.1%	LLL 30.9%	PPO 31.6%	SOS 55%	POS 40.8%	POO 25.0%	LLL 21.9%
OOO 27.9%	SOO 18.7%	LLM 26.1%	LLM 26.1%	POO 24.8%	SOO 32.3%	SOS 29.9%	PPO 14.0%	C_{10}LL 18.6%
POP 17.3%	OOLi 17.00%	LLC_{10} 12.0%	MML 10.5%	PPL 10.2%	POO 3.8%	POP 14.5%	OOO 11.0%	LLM 17.2%
SOO 9.1%	POO 13.5	LLC_8 10.5%	LLC_{10} 9.0%	POL 9.9%	SLO 2.8%	PLS 5.5%	PLO 8.8%	$C_{10}C_{10}$L 14.3%
SSO 1.3%	LiLiLi 2.3%	LLM 10.0%	LLC_8 7.4%	SPO 5.7%	OOS 2.6%	SOO 3.1%	POS 11.2%	LMM 9.6%
SSS 0.8%	PPO 1.76%	MMM 3.1%	MMM 3.7%	PPP 4.8%	POS 1.5%	PLP 2.7%	OOS 8.0%	LMP 4.7%
PPP 0.5%		LLC_6 2.6%-	LLO 2.4%	OOO 4.0%	SSO 1.0%	SLS 1.2%	PPL 4.6%	C_6C_{10}L 3.7%
	--	LLO 1.3%	LLC_6 1.9%	SOO 2.7%	POP 0.4%	OOO 0.7%	OOL 4.2%	LLO 2.0%
LLO 2.4%		LOM 0.9%	LOM 1.7%	PLL 2.1%	SLL 0.3%	--	SSO 3.5%	LPP 1.7%
--	--	LOO 0.8%	MMP 1.2%	OOL 1.6%	OOO 0.3%	--	PPS 2.2%	C_6C_6L 1.0%

From Table 9, AAK and AVK contain similar TAG molecules to those in virgin coconut oil. LLL was the major TAG present in their molecular mixture. Some of the TAGs found in AVP and AAP appear to be present in palm oil, shea butter, cocoa butter and crabwood oil. These similar TAGs include OOO, POO, PPO and SOO.

3.8.2. Melting Point Comparison

Table 10 compares the melting points obtained for AVK and AAK in this work with two well-known and utilized commercial fats, shea butter and cocoa butter.

Table 10. Comparison of AAK and AVK fats melting temperatures with shea butter and cocoa butter.

Physical Properties	AVK	AAK	Shea Butter	Cocoa Butter
Melting (T_p) (°C)	30 ± 1	31 ± 1	37 [62]	29 [63]

The melting temperature of fats (determined by the peak temperature (T_p) of the largest exothermic event of the DSC curve), is a critical parameter in various industries, with particular significance in cosmetics. Fats exhibiting lower melting temperatures are highly sought after for their "melt on skin" effect, which make them excellent emollients. Two of the most well-known examples are shea butter and cocoa butter, which have melting temperatures of 37 °C and 29 °C, respectively, (shown in Table 10). AVK and AAK demonstrate melting temperatures within these ranges, underscoring their potential for application as emollients.

3.8.3. Viscosity and Flow Behavior Comparison

The viscosity and flow behavior of fats and oils are also important parameters to consider. All the fats and oils presented in Table 11 exhibit Newtonian behavior. Materials demonstrating Newtonian behavior maintain a consistent viscosity regardless of changes in shear rate, considering all else equal. This behavior ensures that the performance of these materials remains predictable and uniform. This is important if the fats and oils are to be used in combination with other fats and oil or as viscosity enhancers in other matrices.

Table 11. Comparison of AVK and AAK fats and AVP and AAP oils with shea butter and cocoa butter.

	Fats				Oils			
Physical Properties	**AVK**	**AAK**	**Shea Butter [62]**	**Cocoa Butter [64]**	**AVP**	**AAP**	**Palm Oil [65]**	**Coconut Oil [65]**
Dynamic Viscosity @ 40 °C (mPa·S)	28.29	29.36	46.98	42.30	36.35	35.03	54.80	22.35
Flow Behavior	Newtonian	Newtonian	Newtonian	Newtonian	Newtonian	Newtonian	Newtonian	Newtonian

The dynamic viscosity refers to the force needed by a fluid to overcome its internal molecular friction and is used as a measure of a material's ability to flow. At 40 °C, the dynamic viscosity of AVK and AAK was, on average, 16 mPa·s lower than that of shea butter and cocoa butter but similar to that of coconut oil (22.35 mPa·S). The similarity between the dynamic viscosities of AAK and AVK and coconut oil may be related to their similar lipid profiles, which are predominated by lauric acid. AVP and AAP oils presented lower dynamic viscosities than palm oil, likely owing to their higher relative intensity of unsaturated TAGs (e.g., OOO and POO), as shown in Table 3.

Potential allergenicity and toxicity are important considerations for cosmetic applications. Although one study that examined the toxicity of the AA extract [40] found that these oils are not toxic, there is no definitive answer to this critical question. Astrocaryum oils and fats need to be evaluated for all aspects of allergenicity and toxicity. Further research is required to fully understand their effects on skin health and compatibility with different cosmetic ingredients to ensure formulation safety and efficacy. It is, however, appropriate to

mention that these fats and oils have been consumed for thousands of years by Amazonian and Guyana Shield Indigenous Peoples and that in the states of Amazonia and Roraima in Brazil they are valued exotic foods in mainstream restaurants.

4. Conclusions

This work established the lipid profiles for cold-pressed *Astrocaryum vulgare* (AV) and *Astrocaryum aculeatum* (AA) pulp oils and kernel fats, as well as their crystal packing and microstructures and related these levels of structural organization to their thermal degradation and phase transformation and flow behavior. This work established, for the first time, differences in the molecular profiles of AA and AV pulp oil and kernel fats sourced from Guyana's rainforests and coastal lowlands, respectively, and highlighted important differences to the published information on AVP oil, which was sourced from Brazil instead of Guyana. AAP oil was shown to have unsaturated TAGs, for example 38% OOO and 17% OOL. This is comparable in unsaturation levels to olive oil and makes it a great candidate to be utilized as a nutraceutical edible oil. AVP oil, although significantly more saturated than AAP oil, presents a profile that qualifies it as an excellent liquid frying oil with added nutritional benefits. Both pulp oils present a unique and pleasing flavor profile, which is advantageous to their use in nutraceuticals. The use of the pulp oils in cosmetics is well documented but can likely be optimized through the understanding of the internal structure and physical properties outlined in this work. The AA and AV kernel fats have attributes that make them potential alternatives to shea and cocoa butters in key cosmetic and confectionery applications. Their melting profiles, flow behaviors and microstructures indicate that these are classic plastic fats whose textures and physical properties can be manipulated through processing, blending and interesterification to achieve tailored outcomes. They are also important sources of medium-chain TAGs, specifically lauric and myristic acids, like coconut oil. This suggests these oils as excellent candidates for applications that require solid fats capable of readily melting upon contact, not only in foods but also in dermal applications such as balms and soaps.

Supplementary Materials: The following supporting information can be downloaded at: https://www.mdpi.com/article/10.3390/thermo4010009/s1, Figure S1: Full-scan ESI-MS from 150 to 2000 m/z for (a) *Astrocaryum vulgare pulp* oil, (b) *Astrocaryum Aculeatum* pulp oil, (c) *Astrocaryum vulgare* kernel oil and (d) *Astrocaryum Aculeatum* kernel oil. Major peaks are labeled with the identified molecule adducts; Table S1: Shear rate vs. shear stress data for AVK and AAK; Table S2: Shear rate vs. shear stress data for AVP and AAP; Table S3: Subcell units of the polymorphic forms typical of fatty acid derivatives and their associated characteristic Bragg's d-spacing values and Miller indices.

Author Contributions: Conceptualization, S.D., N.S., L.B. and S.S.N.; Methodology, S.D., N.S., L.B. and S.S.N.; Software, S.D., N.S., L.B. and S.S.N.; Validation, S.D., N.S., L.B., R.J.N.E., S.M. and S.S.N.; Formal analysis, S.D., N.S., L.B. and S.S.N.; Investigation, S.D., N.S., L.B. and S.S.N.; Resources, S.S.N.; Data curation, S.D., N.S., L.B. and S.S.N.; Writing – original draft, S.D., N.S., L.B. and S.S.N.; Writing–review & editing, S.D., N.S., L.B., R.J.N.E., S.M. and S.S.N.; Visualization, S.D., N.S., L.B. and S.S.N.; Supervision, N.S., L.B., R.J.N.E., S.M. and S.S.N.; Project administration, S.S.N.; Funding acquisition, S.S.N. All authors have read and agreed to the published version of the manuscript.

Funding: This research is part of the Sustainable Guyana Program, a partnership between Trent University and the University of Guyana funded by CGX Energy Inc. and Frontera Energy Corporation.

Data Availability Statement: Data is contained within the article or Supplementary Material.

Acknowledgments: The Sustainable Guyana Program, a partnership between Trent University and the University of Guyana funded by CGX Energy Inc. and Frontera Energy Corporation, the Natural Sciences and Engineering Research Council of Canada (NSERC) and Trent University are acknowledged. The experimental contributions of Isidro Ubaldo Espinosa and collaboration with the communities of Surama in Region 9, Guyana and Cabora, Kamwatta and Waramuri in Region 1, Guyana are also acknowledged.

Conflicts of Interest: The authors declare that this study received funding indirectly from CGX Energy Inc. and Frontera Energy Corporation. The funders were not involved in the study design, collection, analysis, interpretation of data, the writing of this article or the decision to submit it for publication.

References

1. Dini, I.; Laneri, S. The New Challenge of Green Cosmetics: Natural Food Ingredients for Cosmetic Formulations. *Molecules* **2021**, *26*, 3921. [CrossRef]
2. Rocca, R.; Acerbi, F.; Fumagalli, L.; Taisch, M. Sustainability paradigm in the cosmetics industry: State of the art. *Clean. Waste Syst.* **2022**, *3*, 100057. [CrossRef]
3. Traversier, M.; Gaslondes, T.; Milesi, S.; Michel, S.; Delannay, E. Polar lipids in cosmetics: Recent trends in extraction, separation, analysis and main applications. *Phytochem. Rev.* **2018**, *17*, 1179–1210. [CrossRef]
4. Bonnet, C. Lipids, a natural raw material at the heart of cosmetics innovation. *OCL* **2018**, *25*, D501. [CrossRef]
5. Rabasco Álvarez, A.M.; González Rodríguez, M.L. Lipids in pharmaceutical and cosmetic preparations. *Grasas Aceites* **2000**, *51*, 74–96. [CrossRef]
6. Kristmundsdóttir, T.; Skúlason, S. Lipids as Active Ingredients in Pharmaceuticals, Cosmetics and Health Foods. In *Lipids and Essential Oils as Antimicrobial Agents*; John Wiley & Sons, Ltd.: Hoboken, NJ, USA, 2011; pp. 151–177.
7. Teixeira, G.L.; Ibañez, E.; Block, J.M. Emerging Lipids from Arecaceae Palm Fruits in Brazil. *Molecules* **2022**, *27*, 4188. [CrossRef] [PubMed]
8. Machado, A.P.d.F.; Nascimento, R.d.P.d.; Alves, M.d.R.; Reguengo, L.M.; Marostica Junior, M.R. Brazilian tucumã-do-Amazonas (*Astrocaryum aculeatum*) and tucumã-do-Pará (*Astrocaryum vulgare*) fruits: Bioactive composition, health benefits, and technological potential. *Food Res. Int.* **2022**, *151*, 110902. [CrossRef] [PubMed]
9. Kahn, F.; Moussa, F. Economic Importance of *Astrocaryum aculeatum* (Palmae) in Central Brazilian Amazonia. *Acta Bot. Venez.* **1999**, *22*, 237–245.
10. Falcao, A.d.O.; Speranza, P.; Ueta, T.; Martins, M. Antioxidant potential and modulatory effects of restructured lipids from the Amazonian palms on liver cells. *Food Technol. Biotechnol.* **2017**, *55*, 553–561. [PubMed]
11. Bezerra, C.V.; Rodrigues, A.; de Oliveira, P.D.; da Silva, D.A.; da Silva, L.H.M. Technological properties of amazonian oils and fats and their applications in the food industry. *Food Chem.* **2017**, *221*, 1466–1473. [CrossRef] [PubMed]
12. Cardona Jaramillo, J.E.; Carrillo Bautista, M.P.; Alvarez Solano, O.A.; Achenie, L.E.K.; González Barrios, A.F. Impact of the Mode of Extraction on the Lipidomic Profile of Oils Obtained from Selected Amazonian Fruits. *Biomolecules* **2019**, *9*, 329. [CrossRef] [PubMed]
13. Burlando, B.; Cornara, L. Revisiting Amazonian Plants for Skin Care and Disease. *Cosmetics* **2017**, *4*, 25. [CrossRef]
14. Mosquera Narvaez, L.E.; Ferreira, L.M.; Sanches, S.; Alesa Gyles, D.; Silva-Júnior, J.O.; Ribeiro Costa, R.M. A Review of Potential Use of Amazonian Oils in the Synthesis of Organogels for Cosmetic Application. *Molecules* **2022**, *27*, 2733. [CrossRef]
15. Ibiapina, A.; Gualberto, L.d.S.; Dias, B.B.; Freitas, B.C.B.; Martins, G.A.d.S.; Melo Filho, A.A. Essential and fixed oils from Amazonian fruits: Proprieties and applications. *Crit. Rev. Food Sci. Nutr.* **2022**, *62*, 8842–8854. [CrossRef] [PubMed]
16. Kahn, F. The genus *Astrocaryum* (Arecaceae). *Rev. Peru. Biol.* **2008**, *15*, 31–48. [CrossRef]
17. Deonarine, S.; Soodoo, N.; Bouzidi, L.; Narine, S.S. Oil Extraction and Natural Drying Kinetics of the Pulp and Seeds of Commercially Important Oleaginous Fruit from the Rainforests of Guyana. *Processes* **2023**, *11*, 3292. [CrossRef]
18. Menezes, E.G.O.; Barbosa, J.R.; Pires, F.C.S.; Ferreira, M.C.R.; de Souza e Silva, A.P.; Siqueira, L.M.M.; de Carvalho Junior, R.N. Development of a new scale-up equation to obtain Tucumã-of-Pará (*Astrocaryum vulgare* Mart.) oil rich in carotenoids using supercritical CO_2 as solvent. *J. Supercrit. Fluids* **2022**, *181*, 105481. [CrossRef]
19. Souza, A.G.; Santos, J.C.O.; Conceição, M.M.d.; Silva, M.C.D.; Prasad, S. A thermoanalytic and kinetic study of sunflower oil. *Braz. J. Chem. Eng.* **2004**, *21*, 265–273. [CrossRef]
20. Silva, M.B.; Perez, V.H.; Pereira, N.R.; Silveira, T.d.C.; da Silva, N.R.F.; de Andrade, C.M.; Sampaio, R.M. Drying kinetic of tucum fruits (*Astrocaryum aculeatum* Meyer): Physicochemical and functional properties characterization. *J. Food Sci. Technol.* **2018**, *55*, 1656–1666. [CrossRef]
21. Craveiro Holanda Malveira Maia, G.; da Silva Campos, M.; Barros-Monteiro, J.; Eduardo Lucas Castillo, J.; Soares Faleiros, M.; Souza de Aquino Sales, R.; Moraes Lopes Galeno, D.; Lira, E.; das Chagas do Amaral Souza, F.; Ortiz, C.; et al. Effects of *Astrocaryum aculeatum* Meyer (Tucumã) on Diet-Induced Dyslipidemic Rats. *J. Nutr. Metab.* **2014**, *2014*, 202367. [CrossRef]
22. Pardauil, J.J.; de Molfetta, F.A.; Braga, M.; de Souza, L.K.; Filho, G.N.; Zamian, J.R.; Da Costa, C. Characterization, thermal properties and phase transitions of amazonian vegetable oils. *J. Therm. Anal. Calorim.* **2017**, *127*, 1221–1229. [CrossRef]
23. Oboh, F.O.J.; Oderinde, R.A. Analysis of the pulp and pulp oil of the tucum (*Astrocaryum vulgare* Mart) fruit. *Food Chem.* **1988**, *30*, 277–287. [CrossRef]
24. de Santana Lopes, A.; Gomes Pacheco, T.; Nascimento da Silva, O.; Magalhães Cruz, L.; Balsanelli, E.; Maltempi de Souza, E.; de Oliveira Pedrosa, F.; Rogalski, M. The plastomes of *Astrocaryum aculeatum* G. Mey. and *A. murumuru* Mart. show a flip-flop recombination between two short inverted repeats. *Planta* **2019**, *250*, 1229–1246. [CrossRef] [PubMed]
25. Santosa, M.; Marmesatb, S.; Britoc, E.; Alvesd, R.; Dobarganesb, M. Major components in oils obtained from Amazonian palm fruits. *Grasas Aceites* **2013**, *64*, 3.

26. dos Santos, O.V.; Pinaffi-Langley, A.C.d.C.; Ferreira, M.C.R.; de Souza, A.L.G.; Carvalho-Junior, R.N.; Teixeira-Costa, B.E. Effect of extraction type on the fatty acids profile and physicochemical properties of biolipids from *Astrocaryum vulgare* pulp: Supercritical CO_2 versus n-hexane extractions. *Int. J. Food Sci. Technol.* **2023**, *58*, 3982–3995. [CrossRef]
27. Mendonça Morais, R.; Roberta Pinheiro Pantoja, K.; Gama Ortiz Menezes, E.; Cristina Seabra Pires, F.; Quaresma da Silva de Aguiar, I.; Cristine Melo Aires, G.; de Freitas Maués de Azevedo, F.; Nunes de Carvalho Junior, R. Tucumã of Pará oil: Chemical profile, biological activities, and methods of extraction. *Peer Rev.* **2023**, *5*, 369–392. [CrossRef]
28. Baldissera, M.D.; Souza, C.F.; Doleski, P.H.; Grando, T.H.; Sagrillo, M.R.; da Silva, A.S.; Leal, D.B.R.; Monteiro, S.G. Treatment with tucumã oil (*Astrocaryum vulgare*) for diabetic mice prevents changes in seric enzymes of the purinergic system: Improvement of immune system. *Biomed. Pharmacoter.* **2017**, *94*, 374–379. [CrossRef] [PubMed]
29. Rodrigues, A.M.; Darnet, S.; Silva, L.H. Fatty acid profiles and tocopherol contents of buriti (*Mauritia flexuosa*), patawa (*Oenocarpus bataua*), tucuma (*Astrocaryum vulgare*), mari (*Poraqueiba paraensis*) and inaja (*Maximiliana maripa*) fruits. *J. Braz. Chem. Soc.* **2010**, *21*, 2000–2004. [CrossRef]
30. Linhares, B.M.; Costa, A.; Abreu, H.D.; Melo, A.; Ribeiro, P.R.; Montero, I.F.; Melo Filho, A.; Santos, R.C. Fatty Acids Profile, Physicalchemical Properties and Minerals with Quantify Indicador of *Astrocaryum aculeatum* Pulp Oil. *J. Agric. Sci* **2017**, *9*, 352. [CrossRef]
31. Bora, P.S.; Narain, N.; Rocha, R.V.M.; De Oliveira Monteiro, A.C.; De Azevedo Moreira, R. Characterisation of the Oil and Protein Fractions of Tucuma (Astrocaryum Vulgare Mart.) Fruit Pulp and Seed Kernel Caracterización de las fracciones Protéicas y Lipídicas de Pulpa y Semillas de Tucuma (Astrocaryum Vulgare Mart.) Caracterización das Fraccións Protéicas e Lipídicas da Pulpa e Semillas de Tucuma (Astrocaryum Vulgare Mart.). *Cienc. Tecnol. Aliment.* **2001**, *3*, 111–116.
32. Didonet, A.A.; Antoniassi, R.; Back, G.R.; de Faria-Machado, A.F.; Wilhelm, A.E.; Ferraz, I.D.K. Characterization of amount and quality of tucuman kernel oil as a potential biomass. *J. Am. Oil Chem. Soc.* **2020**, *97*, 955–962. [CrossRef]
33. Gomes, A.T.A.; Pereira, R.R.; Duarte Junior, A.P.; da Cruz Rodrigues, A.M.; Remédios, C.M.R.; Brasil, D.d.S.B.; Morais, L.R.B.; Silva-Júnior, J.O.C.; Ribeiro-Costa, R.M. Tucumã (*Astrocaryum vulgare*) fat: An Amazonian material as a pharmaceutical input for lipid nanoparticle production. *J. Therm. Anal. Calorim.* **2020**, *147*, 355–365. [CrossRef]
34. Bereau, D.; Benjelloum-Mlayah, B.; Banoub, J.; Bravo, R. FA and unsaponifiable composition of five Amazonian palm kernel oils. *J. Am. Oil Chem. Soc.* **2003**, *80*, 49–53. [CrossRef]
35. Bony, E.; Boudard, F.; Brat, P.; Dussossoy, E.; Portet, K.; Poucheret, P.; Giaimis, J.; Michel, A. Awara (*Astrocaryum vulgare* M.) pulp oil: Chemical characterization, and anti-inflammatory properties in a mice model of endotoxic shock and a rat model of pulmonary inflammation. *Fitoterapia* **2012**, *83*, 33–43. [CrossRef] [PubMed]
36. da Silva Sousa, H.M.; Leal, G.F.; da Silva Gualberto, L.; de Freitas, B.C.B.; Guarda, P.M.; Borges, S.V.; Morais, R.A.; de Souza Martins, G.A. Exploration of the chemical characteristics and bioactive and antioxidant potential of tucumã (*Astrocaryum vulgare*), peach palm (*Bactris gasipaes*), and bacupari (*Garcinia gardneriana*) native Brazilian fruits. *Biomass Convers. Biorefinery* **2023**. [CrossRef]
37. Rossato, A.; da Silva Silveira, L.; Lopes, L.Q.S.; De Sousa Filho, W.P.; Schaffer, L.F.; Santos, R.C.V.; Sagrillo, M.R. Evaluation in vitro of antimicrobial activity of tucumã oil (*Astrocaryum vulgare*). *Arch. Biosci. Health* **2019**, *1*, 99–112. [CrossRef]
38. Nascimento, K.; Copetti, P.M.; Fernandes, A.; Klein, B.; Fogaça, A.; Zepka, L.Q.; Wagner, R.; Ourique, A.F.; Sagrillo, M.R.; da Silva, J.E.P. Phytochemical analysis and evaluation of the antioxidant and antiproliferative effects of Tucumã oil nanocapsules in breast adenocarcinoma cells (MCF-7). *Nat. Prod. Res.* **2021**, *35*, 2060–2065. [CrossRef]
39. Copetti, P.; Oliveira, P.; Vaucher, R.; Duarte, M.; Krause, L. Tucumã extracts decreases PML/RARA gene expression in NB4/APL cell line. *Arch. Biosci. Health* **2019**, *1*, 77–98. [CrossRef]
40. Guex, C.G.; Cassanego, G.B.; Dornelles, R.C.; Casoti, R.; Engelmann, A.M.; Somacal, S.; Maciel, R.M.; Duarte, T.; Borges, W.d.S.; Andrade, C.M.d.; et al. Tucumã (*Astrocaryum aculeatum*) extract: Phytochemical characterization, acute and subacute oral toxicity studies in Wistar rats. *Drug Chem. Toxicol.* **2022**, *45*, 810–821. [CrossRef]
41. Bonadiman, B.; Chaves, C.; Assmann, C.E.; Weis, G.C.C.; Alves, A.O.; Gindri, A.L.; Chaves, C.; da Cruz, I.B.M.; Zamoner, A.; Bagatini, M.D. Tucumã (*Astrocaryum aculeatum*) Prevents Oxidative and DNA Damage to Retinal Pigment Epithelium Cells. *J. Med. Food* **2021**, *24*, 1050–1057. [CrossRef] [PubMed]
42. Uncu, O.; Ozen, B.; Tokatli, F. Use of FTIR and UV–visible spectroscopy in determination of chemical characteristics of olive oils. *Talanta* **2019**, *201*, 65–73. [CrossRef]
43. Nimbkar, S.; Leena, M.M.; Moses, J.A.; Anandharamakrishnan, C. Medium chain triglycerides (MCT): State-of-the-art on chemistry, synthesis, health benefits and applications in food industry. *Compr. Rev. Food Sci. Food Saf.* **2022**, *21*, 843–867. [CrossRef] [PubMed]
44. Heym, F.; Etzold, B.J.M.; Kern, C.; Jess, A. An improved method to measure the rate of vaporisation and thermal decomposition of high boiling organic and ionic liquids by thermogravimetrical analysis. *Phys. Chem. Chem. Phys.* **2010**, *12*, 12089–12100. [CrossRef] [PubMed]
45. Bouzidi, L.; Boodhoo, M.V.; Kutek, T.; Filip, V.; Narine, S.S. The binary phase behavior of 1,3-dilauroyl-2-stearoyl-sn-glycerol and 1,2-dilauroyl-3-stearoyl-sn-glycerol. *Chem. Phys. Lipids* **2010**, *163*, 607–629. [CrossRef] [PubMed]
46. Macridachis, J.; Bayés-García, L.; Calvet, T. Mixing phase behavior of trilaurin and monounsaturated triacylglycerols based on palmitic and oleic fatty acids. *J. Therm. Anal. Calorim.* **2023**, *148*, 12987–13001. [CrossRef]

47. Nagamizu, H.; Miyagawa, Y.; Ogawa, T.; Adachi, S. Phase Behavior of Binary Mixtures of Tripalmitin, Triolein, and Trilinolein. *Food Sci. Technol. Res.* **2020**, *26*, 589–595. [CrossRef]
48. Bouzidi, L.; Narine, S.S. Evidence of critical cooling rates in the nonisothermal crystallization of triacylglycerols: A case for the existence and selection of growth modes of a lipid crystal network. *Langmuir* **2010**, *26*, 4311–4319. [CrossRef] [PubMed]
49. Himawan, C.; Starov, V.; Stapley, A. Thermodynamic & kinetic aspects of fat crystallisation. *Adv. Colloid Interface Sci.* **2006**, *122*, 3–33.
50. Che Man, Y.B.; Haryati, T.; Ghazali, H.M.; Asbi, B.A. Composition and thermal profile of crude palm oil and its products. *J. Am. Oil Chem. Soc.* **1999**, *76*, 237–242. [CrossRef]
51. Marangoni, A.G.; Wesdorp, L.H. *Structure and Properties of Fat Crystal Networks*, 2nd ed.; Taylor & Francis: New York, NY, USA, 2012.
52. Narine, S.S.; Marangoni, A.G. Fractal nature of fat crystal networks. *Phys. Rev. E* **1999**, *59*, 1908–1920. [CrossRef]
53. Marangoni, A.G.; Ollivon, M. Fractal character of triglyceride spherulites is a consequence of nucleation kinetics. *Chem. Phys. Lett.* **2007**, *442*, 360–364. [CrossRef]
54. Hondoh, H.; Ueno, S. Polymorphism of edible fat crystals. *Prog. Cryst. Growth Charact. Mater.* **2016**, *62*, 398–399. [CrossRef]
55. Tchobo, F.P.; Seid, A.M.; Nonviho, G.; Zinsou, R.; Mazou, M.; Djossou, A.J. Physicochemical Variability of Shea Butter (*Vitellaria paradoxa*) from the Regions of Chad. *Am. J. Food Sci. Technol.* **2018**, *6*, 253–257.
56. Segall, S.D.; Artz, W.E.; Raslan, D.S.; Ferraz, V.P.; Takahashi, J.A. Analysis of triacylglycerol isomers in Malaysian cocoa butter using HPLC–mass spectrometry. *Food Res. Int.* **2005**, *38*, 167–174. [CrossRef]
57. Yanty, N.; Marikkar, J.; Abdulkarim, S. Determination of types of fat ingredient in some commercial biscuit formulations. *Int. Food Res. J.* **2014**, *21*, 277.
58. Cabral, E.C.; da Cruz, G.F.; Simas, R.C.; Sanvido, G.B.; Gonçalves, L.d.V.; Leal, R.V.; da Silva, R.C.; da Silva, J.C.; Barata, L.E.; da Cunha, V.S. Typification and quality control of the Andiroba (*Carapa guianensis*) oil via mass spectrometry fingerprinting. *Anal. Methods* **2013**, *5*, 1385–1391. [CrossRef]
59. James, S.O.; Bouzidi, L.; Emery, R.J.N.; Narine, S.S. Lipid Fractionation and Physicochemical Characterization of Carapa guianensis Seed Oil from Guyana. *Processes* **2023**, *11*, 2565. [CrossRef]
60. Reyes-Hernández, J.; Dibildox-Alvarado, E.; Charó-Alonso, M.A.; Toro-Vazquez, J.F. Physicochemical and Rheological Properties of Crystallized Blends Containing trans-free and Partially Hydrogenated Soybean Oil. *J. Am. Oil Chem. Soc.* **2007**, *84*, 1081–1093. [CrossRef]
61. Kumar, P.P.; Krishna, A.G. Physicochemical characteristics of commercial coconut oils produced in India. *Grasas Aceites* **2015**, *66*, e062.
62. Abdul-Hammed, M.; Jaji, A.O.; Adegboyega, S.A. Comparative studies of thermophysical and physicochemical properties of shea butter prepared from cold press and solvent extraction methods. *J. King Saud Univ. Sci.* **2020**, *32*, 2343–2348. [CrossRef]
63. Colella, M.F.; Marino, N.; Oliviero Rossi, C.; Seta, L.; Caputo, P.; De Luca, G. Triacylglycerol Composition and Chemical-Physical Properties of Cocoa Butter and Its Derivatives: NMR, DSC, X-ray, Rheological Investigation. *Int. J. Mol. Sci.* **2023**, *24*, 2090. [CrossRef] [PubMed]
64. Landfeld, A.; Novotna, P.; Strohalm, J.; Houska, M.; Kyhos, K. Viscosity of cocoa butter. *Int. J. Food Prop.* **2000**, *3*, 165–169. [CrossRef]
65. Tangsathitkulchai, C.; Sittichaitaweekul, Y.; Tangsathitkulchai, M. Temperature effect on the viscosities of palm oil and coconut oil blended with diesel oil. *J. Am. Oil Chem. Soc.* **2004**, *81*, 401–405. [CrossRef]